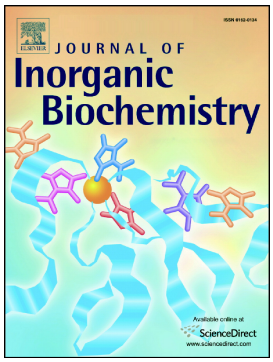

The PmoB subunit of particulate methane monooxygenase (pMMO) in Methylococcus capsulatus (Bath): The CuI sponge and its function

Yu-Jhang Lu, Mu-Cheng Hung, Brian T.-A. Chang, Tsu-Lin Lee, Zhi-Han Lin, I-Kuen Tsai, Yao-Sheng Chen, Chin-Shuo Chang, Yi-Fang Tsai, Kelvin H.-C. Chen, Sunney I. Chan, Steve S.-F. Yu

PII: S0162-0134(18)30516-6
DOI: https://doi.org/10.1016/j.jinorgbio.2019.04.005
Reference: JIB 10691

To appear in: *Journal of Inorganic Biochemistry*

Received date: 2 September 2018
Revised date: 28 February 2019
Accepted date: 8 April 2019

Please cite this article as: Y.-J. Lu, M.-C. Hung, B.T.-A. Chang, et al., The PmoB subunit of particulate methane monooxygenase (pMMO) in Methylococcus capsulatus (Bath): The CuI sponge and its function, Journal of Inorganic Biochemistry, https://doi.org/10.1016/j.jinorgbio.2019.04.005

The PmoB Subunit of Particulate Methane Monooxygenase (pMMO) in *Methylococcus capsulatus* (Bath): The Cu^{I} Sponge and its Function

Yu-Jhang Lu,[a,b,†] Mu-Cheng Hung,[a,c,d,†] Brian T.-A. Chang,[a,e] Tsu-Lin Lee,[a,f] Zhi-Han Lin,[a] I-Kuen Tsai,[a,g] Yao-Sheng Chen,[a] Chin-Shuo Chang,[a] Yi-Fang Tsai,[a] Kelvin H.-C. Chen,[g] Sunney I. Chan,[a,h*] and Steve S.-F. Yu[a,b,c,i*]

From the [a]Institute of Chemistry, Academia Sinica, Taipei 11529, Taiwan
[b]Genetics and Genomics Ph.D. Graduate Program, Academia Sinica and National Chung Hsing University, Taichung 40227, Taiwan
[c]Chemical Biology and Molecular Biophysics Program, Taiwan International Graduate Program (TIGP), Academia Sinica, Taipei 11529, Taiwan
[d]Institute of Biochemical Sciences, National Taiwan University, Taipei 10617, Taiwan
[e]Department of Chemistry, National Tsing-Hua University, Hsinchu 30013, Taiwan
[f]Graduate Institute of Applied Science and Technology, National Taiwan University of Science and Technology, Taipei 10607, Taiwan
[g]Department of Applied Chemistry, National Pingtung University, Pingtung 90003, Taiwan
[h]Division of Chemistry and Chemical Engineering, California Institute of Technology, Pasadena, CA 91125, USA
[i]Department of Chemistry, National Cheng Kung University, Tainan 70101, Taiwan

*corresponding authors: (Steve S.-F. Yu) E-mail: sfyu@gate.sinica.edu.tw; phone number: +886-2-5572-8650; fax number: +886-2-2783-1237 and (Sunney I. Chan) E-mail: sunneychan@yahoo.com; phone number: +886-2-5572-8654; fax number: +886-2-2783-1237
[†]These authors contribute equally to this work.

The contributions of the coauthors to this article are: Y.-J.L., Z.-H.L., T.-L.L. and Y.-S.C. constructed and designed the expression vectors for protein expression; M.-C.H., C.-S.C. and Y.-S.C. conducted the mutagenesis studies; Y.-J.L., M.-C.H., B.T.-A.C. and C.-S.C. carried out the specific activity measurements on the recombinant PmoB constructs; B.T.-A.C. purified the MBP-$PmoB_{55-414}$; Y.-J.L., B.T.-A.C., Y.-F.T. and S.S.-F.Y. conducted the EPR and/or XAS experiments; M.-C.H., B.T.-A.C., Z.-H.L., I.-K.T., C.-S.C. and Y.-S.C. performed the quantification of the copper contents in the proteins, and the protein quantification using antibodies; B.T.-A.C., Z.-H. L., I.-K.T. and C.-S.C. grew the *E. coli* cells for the biochemical and biophysical characterization of the recombinant proteins; K.H.-C.C., S.S.-F.Y. and S.I.C. designed the research; S.S.-F.Y. and S.I.C. wrote the paper.

Highlights

- Subunit B (PmoB) of particulate methane monooxygenase (pMMO) is expressed in *E. coli.*
- PmoB and its variants/mutants are expressed in the membranes as Cu^{I} proteins.
- The PmoB of pMMO contains a Cu^{I} sponge with high reduction potentials for the Cu sites.
- The PmoB proteins show evidence of a dinuclear copper site.
- The PmoB-enriched *E. coli* membranes produce H_2O_2.

ABSTRACT

In this study, we describe efforts to clarify the role of the copper cofactors associated with subunit B (PmoB) of the particulate methane monooxygenase (pMMO) from *Methylococcus capsulatus* (Bath) (*M. capsulatus*). This subunit exhibits strong affinity towards Cu^{I} ions. To elucidate the high copper affinity of the subunit, the full-length PmoB, and the *N*-terminal truncated mutants $PmoB_{33–414}$ and $PmoB_{55–414}$, each fused to the maltose-binding protein (MBP), are cloned and over-expressed into *E. coli* K12 TB1 cells. The Y374F, Y374S and M300L mutants of these protein constructs are also studied. When this *E. coli* is grown with the *pmoB* gene in 1.0 mM Cu^{II}, it behaves like *M. capsulatus* (Bath) cultured under high copper stress with abundant membrane accumulation and high Cu^{I} content. The recombinant PmoB proteins are verified by Western blotting of antibodies directed against the MBP sub-domain in each of the copper-enriched PmoB proteins. X-ray Cu *K*-edge absorption near edge spectroscopy of the copper ions confirms that all the PmoB recombinants are Cu^{I} proteins. All the PmoB proteins show evidence of a “dicopper site” according to analysis of the Cu X-ray absorption extended edge fine structure of the membranes. No specific activities toward methane and propene oxidation are observed with the recombinant membrane-bound PmoB proteins. However, significant production of hydrogen peroxide is observed in the case of the $PmoB_{33-414}$ mutant. Reaction of the dicopper site with dioxygen produces hydrogen peroxide and leads to oxidation of the Cu^{I} ions residing in the C-terminal sub-domain of the PmoB subunit.

Keywords

copper sites; particulate methane monooxygenase─(pMMO); membrane protein; methane oxidation; oxygen/hydrogen-peroxide redox loop; X-ray absorption spectroscopy.

1. INTRODUCTION

The particulate methane monooxygenase (methane monooxygenase (particulate), (EC 1.14.18.3), pMMO) is a membrane-bound metalloenzyme that converts methane into methanol in methanotrophs under ambient conditions of temperature and pressure [1−8]. With a K_m of ~0.1 μM for methane and a V_{max} approaching one molecule of methane oxidized per sec per enzyme molecule, it is the most efficient methane oxidizer known [9]. As the central enzyme in C1 metabolism in methanotrophic bacteria, pMMO has become the paradigm for developing an understanding of the chemistry discovered by Nature to accomplish efficient selective methane oxidation under ambient conditions. This complex protein consists of three subunits (PmoA, PmoB, and PmoC) and many copper cofactors [1−3, 6−8, 10]. The functioning of the enzyme requires as many as 12−15 copper ions [1, 2, 6, 10−12]. The catalytic site appears to be a reduced tricopper cluster ($Cu^ICu^ICu^I$) that becomes functional upon activation with O_2 [6, 10, 11−13], although mononuclear copper and dicopper centers have also been proposed [7, 14-16]. The enzyme is expected to contain additional cofactors for the input and storage of electrons as well as to gate or control the flow of reducing equivalents to the catalytic site to mitigate futile cycles [6, 17].

Crystal structures of pMMO from *Methylococcus capsulatus* (Bath) (*M. capsulatus* (Bath)) [7] (Fig. 1), *Methylosinus trichosporium OB3b* [15] and *Methylocystis* species

strain M [18] have revealed no more than three or four copper ions: two mononuclear copper centers and a dinuclear copper site. The mononuclear copper is located at the **A** and **C** sites in the protein, and the dicopper center at the **B** site (see Fig. 1 for location of these metal sites in the crystal structure). However, biochemical and biophysical studies have provided evidence for a tricopper cluster [6, 10−13], and recently, a tricopper-peptide complex based on the short helix that lines the empty hydrophilic cavity at the **D** site has been demonstrated to mediate efficient conversion of methane into methanol as well as epoxidation of propene to propylene oxide [19] (see Fig. 1 for location of the putative tricopper cluster). Additional copper ions are also associated with the *C*-terminal sub-domain of the PmoB subunit [20]. These copper ions have unusually high reduction potentials and are typically reduced; they are also inert toward O_2 [6, 10, 11]. It has been suggested that these copper ions provide a reservoir of reducing equivalents to re-reduce the tricopper cluster of the proposed active site after the latter cofactor has completed the oxidative phase of the enzyme turnover [6, 10−13]. For this reason, this group of Cu^I ions has been referred to as "E-clusters" to denote their possible role as a supplier of reducing equivalents to restore the tricopper cluster at the active site (C-cluster) to their functional redox state (Cu^I) after substrate oxidation has been accomplished [6, 10−13].

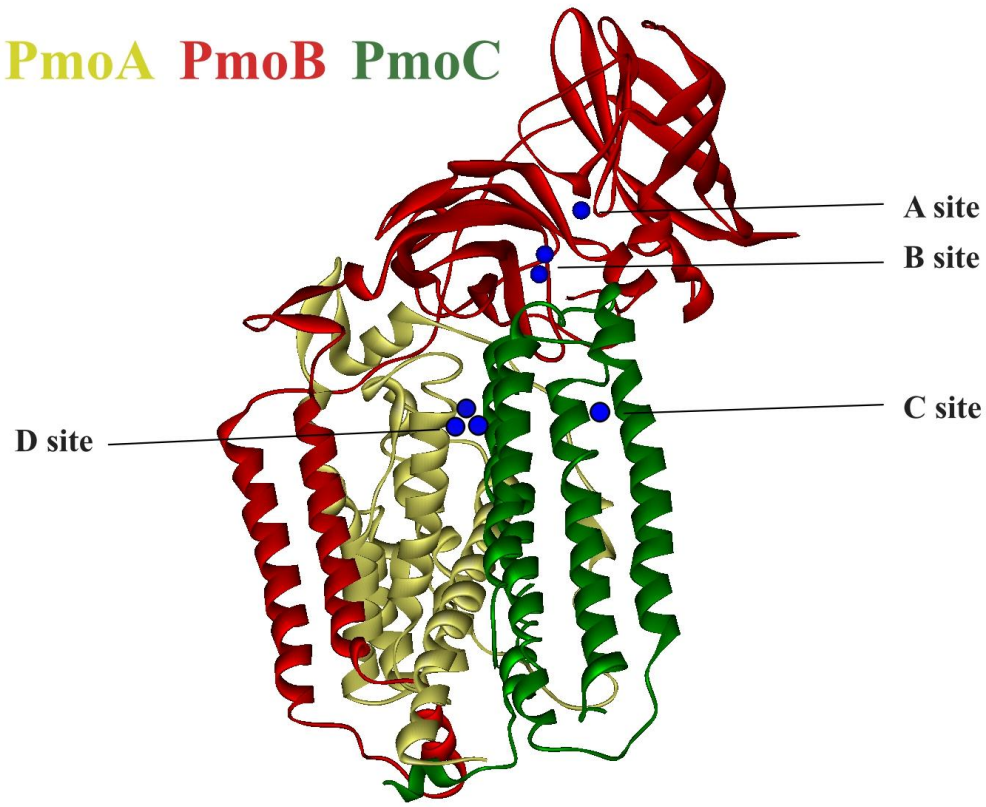

Fig. 1. X-ray crystal structure of pMMO from *M, capsulatus* (Bath). The membrane topology of the PmoB subunit (*red*) is highlighted *vis a vis* the PmoA (*yellow*) and PmoC (*green*) subunits. The locations of the known copper sites are shown by *blue* atoms: **A** site (mononuclear copper site); **B** site (dicopper site); **C** site ("zinc" center or second mononuclear copper site); and **D** site (the site of the putative tricopper cluster described by the Chan laboratory [6, 10−13]).

Unlike the PmoA and PmoC subunits of pMMO, which are mostly embedded in the bilayer membrane, the PmoB subunit is only anchored in the membrane by a short stretch of two transmembrane helical segments (*ca.* 70 residues) flanked by two large water-soluble sub-domains (Fig. 1). Together with PmoA and PmoC, this subunit forms part of the massive transmembrane helix bundle of the assembled pMMO protein complex in the lipid bilayer [7]. The *N*-terminal and *C*-terminal sub-domains rest on the membrane-aqueous interface in contact with the cytoplasmic surface of the membrane,

interacting with each other, as well as with the PmoA and PmoC subunits, not to mention redox protein partners and other substrates in the cytoplasm of the cell.

It has been known for some years that the pMMO from *M. capsulatus* (Bath) contains as many as 12−15 copper ions if the protein is purified under anaerobic conditions [1-3, 11, 20]. When the Cu^{I} enzyme solubilized in detergent is purified by chromatography in air, some of the copper ions become oxidized and can be stripped off from the protein [3, 10, 11]. Surprisingly, the bulk of the copper ions of the enzyme are associated with the PmoB subunit [10, 11, 20]. Clearly, with so many copper centers distributed among the three protein subunits, the study of this membrane system is extremely challenging. A strategy has been developed to dissect the problem into functional domains. As effectiveness of this strategy, we have recently identified and studied a hydrophilic construct embodying a tricopper cluster site sequestered within the transmembrane domain of the PmoA and PmoC subunits and demonstrated that a tricopper peptide complex prepared from the amino acid residues of this peptide is capable of mediating facile methane oxidation as well as propene epoxidation when the $Cu^{I}Cu^{I}Cu^{I}$ tricopper cluster is activated by O_2 under ambient conditions [19].

Using this same approach, we have cloned and over-expressed the water-soluble *apo N*-terminal and *C*-terminal sub-domains of the PmoB subunit individually in *Escherichia coli* (*E. coli*) and showed that the *C*-terminal sub-domain is a Cu^{I}-sponge, sequestering as many as 10 Cu^{I} ions [20]. The binding of the Cu^{I} ions was found to be cooperative. Interestingly, Cu^{II} ions exhibit very low affinity for this sub-domain, suggesting that it is necessary to involve copper transport/trafficking proteins (or copper chaperones) to incorporate these copper ions into this region of the PmoB subunit for

proper assembly of the native protein fold [3]. In our earlier work, the *N*-terminal sub-domain was expressed only as an inclusion body. It was subsequently expressed with a glutathione S-transferase tag and the solubilized protein was shown to be capable of binding 3–4 copper ions, either Cu^{II} or Cu^{I} (data not published). Thus, there is no question that many copper ions of pMMO are associated with the PmoB subunit.

On the other hand, following a similar strategy, Rosenzweig *et al*. [14] have reported a recombinant soluble variant (spmoB) of the PmoB *N*-terminal soluble fragment (residues 33–172) containing both the **A** and **B** sites tethered to the *C*-terminal fragment (residues 265–414) by a Gly-Lys-Gly-Gly-Gly (GKGGG) linker. This PmoB recombinant variant was demonstrated to coordinate a total of three copper ions. To obtain the *holo* spmoB, these researchers added $CuSO_4$ to the *apo* form of the recombinant protein to obtain the three-copper spmoB after purification accordingly. To clarify the differences between these results and our earlier findings, we have now cloned and over-expressed the full-length PmoB and two *N*-truncated PmoB subunits, as well as several of their mutants in a copper tolerant strain of *E. coli*, under conditions in which copper transport/trafficking proteins are available to ensure insertion of these copper ions during biosynthesis and proper assembly and folding of the membrane-bound PmoB proteins [21−23]. Indeed, we find that many Cu^{I} ions are associated with the PmoB proteins expressed in these *E. coli* membranes. Here, we describe biophysical characterization of these copper ions in the various PmoB constructs to clarify the number of copper ions, their redox state(s), and their reactivity toward O_2 and ferricyanide ($[Fe(CN)_6]^{3-}$). Armed with these results, and together with our recent finding that the catalytic site is most likely buried at the interface between

the PmoA and PmoC subunits in the transmembrane domain of the protein complex [13, 19, 24], we can begin to understand the role played by these copper ions of the PmoB subunit in the catalytic cycle of the *holo* enzyme.

2. MATERIALS AND METHODS

2.1 Bacterial strains, plasmids, and growth conditions

E. coli strains DH5α (Yeastern Biotech) and K12 TB1 (New England Biolabs), and plasmids pET 21b (Novagen) and pMAL^{TM}-p2X (New England Biolabs) were used for DNA manipulations and protein over-expressions. They were grown in Lucia-Bertani medium (LB medium) in the presence of ampicillin (50 μg/mL). The growth of *M. capsulatus* (Bath) (ATCC 33009) was carried out following the procedures established by Chan *et al.* [1, 2] on nitrate mineral salts medium (NMS buffer, ATCC buffer).

2.2 Construction of the expression plasmids pMAL-p2X(pmob) and pMAL-p2X(deSPpmob1 & deSPpmob2)

The genomic DNA of *M. capsulatus* (Bath) was obtained by following published procedures [19]. The sequences of *pmob* (coding for amino acid residues 1−414), *deSPpmob1* (coding for amino acid residues 33−414, namely, without the signal sequence 1−32), and *deSPpmob2* (coding for amino acid residues 55−414, namely, without the signal sequence and with further truncation of the *N*-terminal domain) were

amplified from the corresponding extracted *M. capsulatus* (Bath) genomic DNA. The twelve primers for *pmob*, *deSPpmob1,* and *deSPpmob2* are:

pmob-f1: 5´AATTCATGAAAACAATAAAGGACCGGA3´;

pmob-f2: 5´CATGAAAACAATAAAGGACCGGATTG 3´;

pmob-r1: 5´TTTACATGAACGACGGGATCAG3´;

pmob-r2: 5´AGCTTTTACATGAACGACGGGAT3´;

deSPpmob1-f1:

5´CGCGGATCCCACGGTGAGAAATCGCAGGCCGCGTT3´;

deSPpmob1-f2: 5´GGATCCCACGGTGAGAAATCGCAGGCC3´;

deSPpmob1-r1: 5´TTTACATGAACGACGGGATCAG 3´;

deSPpmob1-r2: 5´AGCTTTTACATGAACGACGGGAT 3´;

deSPpmob2-f1: 5´AATTCTGGTCGAAAGAGAAAGTCAAG 3´;

deSPpmob2-f2: 5´CTGGTCGAAAGAGAAAGTCAAG 3´;

deSPpmob2-r1: 5´TTTACATGAACGACGGGATCAG 3´; and

deSPpmob2-r2: 5´AGCTTTTACATGAACGACGGGAT 3´.

These primers, together with *pfu* turbo DNA polymerase (Stratagene), were used in the polymerase chain reactions. pMAL^{TM}-p2X was digested by *EcoR* I and *Hind* III (New England Biolabs, Inc.) and ligated with the PCR products by T4 DNA ligase. The three resultant recombinant plasmids, pMAL-p2X(*pmob*) and pMAL-p2X(*deSPpmob1 & deSPpmob2*) were amplified by *E. coli* DH5α and established by sequence analysis. Since each of the target genes is fused to the 3´-end of the maltose-binding protein

(MBP) gene by an intervening linker coding for the 24 amino-acid sequence NSSSNNNNNNNNNNLGIEGRISEF, which includes the Factor Xa cutting site (IEGR), the MBP tag can be excised from each of the PmoB proteins in various experiments, including the preparation of antibodies.

In addition to the *pmob* genes coding for the full-length PmoB, $PmoB_{33–414}$, and $PmoB_{55–414}$ proteins, we have cloned the genes encoding the full-length PmoB Y374F mutant, the *N*-terminal truncated $PmoB_{33–414}$Y374F mutant, and the Y374F, Y374S and M300L mutants of the $PmoB_{55–414}$ protein. To generate the Y374F, Y374S, and M300L mutant proteins, the corresponding *pmob* target genes were site-directed mutated in the recombinant plasmids pMAL-p2X(*pmob*, *deSPpmob1* or *deSPpmob2*). The six primers for Y374F, Y374S, and M300L are:

Y374F-f1: 5'GCGGCGTGGGAAGTGTTCCGTCTGTC3';

Y374F-r1: 5'GACAGACGGAACACTTCCCACGCCGC3';

Y374S-f1: 5'CGGCGTGGGAAGTGAGCCGTCTGTCCGACA3';

Y374S-r1: 5'TGTCGGACAGACGGCTCACTTCCCACGCCG3';

M300L-f1: 5'CCGCGCCATGCGGTTGAAGCTGACCAT3'; and

M300L-r1: 5'ATGGTCAGCTTCAACCGCATGGCGCGG 3'.

Otherwise, the same procedures were used to produce the site-directed *pmob* mutant plasmids as described earlier.

A list of the target PmoB proteins is shown in Table 1. The protein construct for the full-length PmoB fused to the MBP is illustrated in Fig. 2.

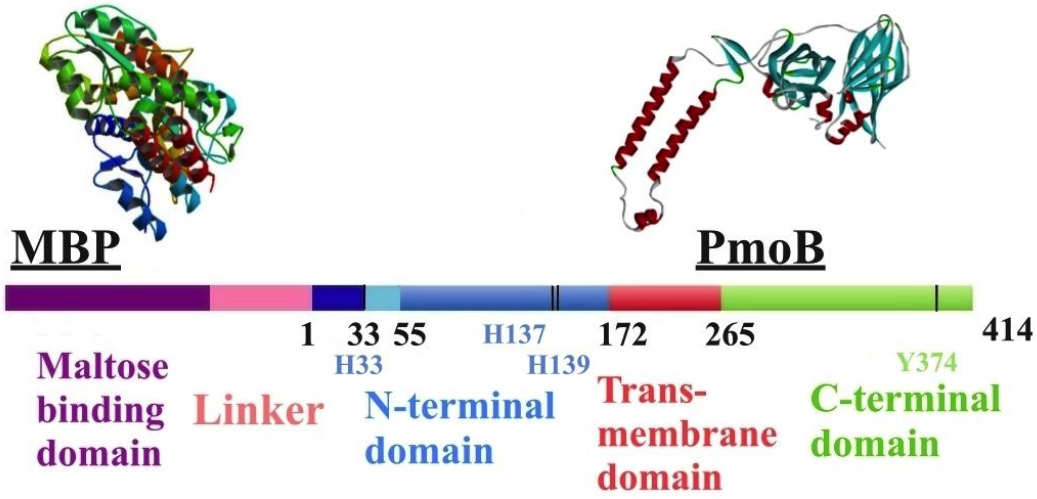

Fig. 2. The protein construct for the full-length PmoB fused to MBP. The *N*- and *C*-terminal sub-domains of the PmoB are highlighted in *blue* and *green*, respectively, with the signal peptide (residues 1 - 32) colored in *deep blue*, and the transmembrane domain from residues 172 to 265 depicted in *red*. The linker between the MBP and the PmoB containing the Factor Xa cleavage site is shown in *magenta*.

Table 1. List of the target PmoB proteins.

PmoB proteins	**Description**
PmoB	The full length PmoB protein
PmoB Y374F	The full length PmoB mutant with Tyr374→Phe
$PmoB_{33–414}$	*N*-truncated PmoB w/o residues 1−32
$PmoB_{33–414}$ Y374F	*N*-truncated PmoB mutant w/o residues 1−32 and Tyr 374→Phe
$PmoB_{55–414}$	*N*-truncated PmoB w/o residues 1−54

$PmoB_{55–414}$ Y374F	*N*-truncated PmoB mutant w/o residues 1−54 and Tyr374→Phe
$PmoB_{55–414}$ Y374S	*N*-truncated PmoB mutant w/o residues 1−54 and Tyr374→Ser
$PmoB_{55–414}$ M300L	*N*-truncated PmoB mutant w/o residues 1−54 and Met300→Leu

2.3 Raising polyclonal antibodies against the recombinant $PmoB_{55–414}$ protein

Polyclonal antibodies against the PmoB subunit were raised in rabbit by GeneTex Inc., Taipei. Polyclonal antiserum was obtained by injecting rabbits with the copper-enriched $PmoB_{55–414}$ protein**.** (Each protein contains *ca*. 5 copper ions (*vide infra*).) The first immunal injection consisted of the purified $PmoB_{55–414}$ protein (0.5 mg) and lipopolysaccharide (1:1 volume); only purified $PmoB_{55–414}$ protein was used in subsequent burst injections. Purification of the polyclonal antibodies was carried out by the affinity purification approach. Series dilution was used to determine the limits of detection in the antibody titer tests.

2.4 Western blotting with rabbit anti-$PmoB_{55–414}$ antibodies (polyclonal) and anti-MBP monoclonal antibody/HRP conjugates

2.4.1 Method 1

The pMMO in the membranes of *M. capsulatus* (Bath), the recombinant $PmoB_{55–414}$ proteins in the membrane pellets, and purified pMMO [2] were analyzed by 12% SDS-PAGE and then transferred to polyvinylidene difluoride (PVDF) membranes. The membranes were blocked with 5% skim milk for 12 h at 4°C and then incubated with rabbit *anti*-$PmoB_{55–414}$ antibodies (1:40,000) and supplemented with a second antibody, the commercial goat *anti*-rabbit immunoglobin antibody (Sigma) conjugated with alkaline phosphatase (1:20,000), to spot the MBP-$PmoB_{55–414}$ fusion-protein in the PVDF membranes. After hybridization at room temperature for 1 h, the membranes were washed by 3 × 25 mL phosphate buffered saline (PBS, pH 7.4, 137 mM NaCl, 2.7 mM KCl, 10 mM Na_2HPO_4 and 2.0 mM KH_2PO_4), and incubated with the alkaline phosphatase substrate, nitro-blue tetrazolium chloride/5-bromo-4-chloro-3'-indolylphosphate *p*-toluidine salt (NBT/BCIP, Thermo Scientific™ Pierce) for the identification of the PmoB subunit (purple-black precipitate). After separation of the pMMO subunits on SDS-PAGE, the subunit B of pMMO could be also identified in this manner without any specialized equipment for visualization. Both the PmoB subunit isolated from the *holo* pMMO and the recombinant $PmoB_{55–414}$ were readily recognized on SDS-PAGE by the rabbit anti-PmoB antibodies, with molecular weights of 45 and 98 kDa, respectively. The pre-stained protein markers used in the SDS-PAGE were obtained from EZColor II™ Prestained Protein Marker (EZ BioResearch LLC).

2.4.2 Method 2

The proteins in the membrane pellets were separated by 10% SDS-PAGE. Proteins on the poly-acrylamide gel were transferred to 0.45 μm Hybond-P hydrophobic PVDF membranes (GE Healthcare), and the membranes were blocked by 5.0% skim milk/TBS (blocking solution) at room temperature for 2.0 h. After blocking, the PVDF membranes were washed with 1.0% skim milk/TBS and then incubated with *anti*-MBP monoclonal antibody, horseradish peroxidase (HRP) conjugates (New England Biolabs, Inc.) in 1/5000 dilution at room temperature for 1.0 h. Before enhanced chemiluminescence (ECL) analysis, the PVDF membranes were washed with TBST (TBS containing 0.10% (v/v) Tween™ 20) three times. HRP substrate (Immobilon™ Western, Millipore, Corp.) was then added to the PVDF membranes and the target proteins spotted by the luminescence were detected using a CCD camera (BioSpectrum® AC Imaging System, UVP, Inc.).

For quantitation of the recombinant target full-length MBP-PmoB, MBP-PmoB$_{33–414,}$ and MBP-PmoB$_{55–414}$ proteins expressed in the *E. coli* K12 TB1 cells, including the various mutant proteins studied, we determined the protein concentrations in the various membranes by Western blotting following the established protocol [25]. MBP5 protein (New England Bioslabs®, Inc.) was used to set up the calibration curve.

2.5 Immunogold labeling of rabbit anti-PmoB antibodies for TEM imaging

E. coli K12 TB1 cells containing the over-expressed MBP-PmoB$_{55–414}$ in section slides were etched by 100% ethanol for 10 min and then incubated with 10 mM EDTA (pH 8.0) for 24 h at 65°C. After washing by PBS, we blocked the section slides using 1% BSA. These slides were then immersed in PBS solution for more than 30 min. Rabbit *anti*-PmoB antibody (1:4000 dilution) was used to hybridize the cells over night at 4°C. After a series of washing with high salt Tween-20 buffer (0.05 M Tris·HCl (pH 7.5), 0.5 M NaCl, 0.1% Tween-20) and PBS solution, we hybridized the bacterial cells in the slides with goat *anti*-rabbit immunoglobin antibody conjugated with gold nanoparticles. The section slides were then fixed by 1% glutaraldehyde, washed by de-ionized water and subjected to transmission electron microscopy (TEM) observation on a *Hitachi H-7000 transmission electron microscope.*

2.6. Determination of the copper contents in the E. coli membranes of the MBP-PmoB fusion proteins by ICP-OES

Aliquots (0.2 mL) of protein samples were dissolved in 4.8 mL of saturated 65% HNO_3 solution (suprapure grade, Merck). The samples were digested in a MARS5 microwave digestion system (CEM Inc.). The temperature was stepped up incrementally from room temperature to 180°C in 15 min, and maintained at 180°C for another 15 min. The process of nitrate digestion was then terminated as the temperature was gradually lowered down to room temperature.

The digested samples were then diluted with 20 mL doubly distilled water (Millipore) prior to copper analysis. The copper contents of the digested samples were determined by Inductively Coupled Plasma-Optical Emission Spectrometry (ICP-OES)

on a Varian 720-ES (Agilent Technology). The copper concentrations of the samples were determined by interpolating a linear plot of a series of standard solutions of $Cu(NO_3)_2$ in 0.10 N HNO_3. A solution of 0.10 N HNO_3 in distilled water was used as the copper-free control.

2.7 Quantification of the level of Cu^I in the E. coli membranes of the MBP-PmoB fusion proteins

Cu^I concentrations were determined spectrophotometrically using bicinchoninic acid (disodium salt, Sigma Inc.) (BCA) [26]. A large amount of BCA (20 mM) was added to the protein sample in order to shift the Cu^I binding equilibrium from the expressed protein to BCA. Under these conditions, all the Cu^I bound to the protein would be stripped off and become bound to the dye. The absorbance of the Cu^I-BCA complex obtained by ascorbate reduction of copper sulfate in the presence of BCA was used as a standard and shown to follow a linear correlation with Cu^I concentration in accordance with the Beer-Lambert's law in the range 10–100 μM Cu^I at the wavelength of 562 nm (r^2 = 0.99). No chromophoric absorption was observed in the presence of Cu^{II}, or in the absence of metal ions, upon the addition of BCA.

2.8 Purification and characterization of the expressed MBP-$PmoB_{55–414}$ fusion protein and the target $PmoB_{55–414}$ protein

The membrane pellets obtained for the *E. coli* cells grown with the recombinant

plasmid pMAL-p2X*deSPpmob2* were re-suspended in TBS buffer (Tris buffer saline composed of 20 mM Tris-HCl, pH 7.4 and 200 mM NaCl) containing 10 mM sodium ascorbate and 0.5% *n*-dodecyl-β-D-maltoside (DDM) for 30 min at 4°C. The membrane solution was ultra-centrifuged (100,000 × *g*, 60 min, 4°C) again, and then was collected and filtrated through 0.45 μm filter. The target fusion proteins were absorbed on to an amylose resin column (New England Bioslabs®, Inc.) in TBS buffer containing 10 mM sodium ascorbate and 0.05% DDM, and were subsequently eluted with the same buffer containing 10 mM maltose.

To remove the MBP tag in the MBP-PmoB$_{55–414}$ protein, a 49 μL purified recombinant protein MBP-PmoB$_{55–414}$ (1 mg/mL) was mixed with 1.0 μL Factor Xa (1 mg/mL, New England BioLab) and incubated overnight at 4°C. The obtained PmoB$_{55–414}$ was eluted through an amylose resin column (New England Bioslabs®, Inc.) by TBS buffer containing 10 mM sodium ascorbate and 0.05% DDM.

The amount of the purified recombinant PmoB$_{55–414}$ protein was identified by the detergent-compatible DC Protein Assay (Bio-Rad). The copper content of the purified PmoB$_{55–414}$ protein was determined by ICP-OES in exactly the same manner as for the purified *E. coli* membranes of the various MBP-PmoB fusion proteins, as described earlier.

2.9 Other experimental procedures and methods

The experimental procedures for the growth of *E. coli* for heterogeneous expression of recombinant PmoB variants; preparation of the periplasmic fraction of *E. coli*;

procedures for the isolation and purification of the *E. coli* membranes; quantification of the total membrane proteins from the *E. coli* cytosolic membranes; activity assays of the recombinant MBP-PmoB proteins in the membranes; measurements of hydrogen peroxide production; ferricyanide titrations; electron paramagnetic resonance (EPR) spectroscopy of the copper ions; and X-Ray absorption spectroscopy (XANES and EXAFS) experiments are given in the "Materials and Methods" section (S.1-S.9) of Supplementary Information.

3. RESULTS

3.1 Expression of the MBP-PmoB fusion proteins in the E. coli membranes

Following standard procedures, we clone the fusion genes of the target PmoB proteins with MBP in plasmids and express the MBP-PmoB proteins in *E. coli* K12 TB1 cells. To assist with the identification of the expressed target PmoB proteins and to determine the levels of expression of these proteins, we have resorted to Western blotting using anti-MBP monoclonal antibody/HRP conjugates. Expression of the MBP-PmoB fusion proteins is detected only in the membranes. There is no indication of any protein expression in the periplasm.

In addition, we have prepared antibodies to the recombinant $PmoB_{55\text{-}414}$ with the bound Cu^{I} ions. These antibodies allow us to identify the $PmoB_{55\text{-}414}$ domain of the expressed PmoB proteins within the bacterial cells or by SDS-PAGE *via* the Western blotting technique (Fig. 3). To obtain the desired antibodies, we first remove the MBP

fusion tag from the MBP-PmoB$_{55-414}$ protein purified from *E. coli* K12 TB1 cells by cleavage with factor Xa. Antiserum is then obtained by injection of the PmoB$_{55-414}$ (copper content 5.12 ± 0.45 per unit protein (*vide infra*)) into the rabbit. In Western blotting experiments, we find that the polyclonal antibodies obtained exhibit high affinity toward the PmoB domain of the recombinant MBP-PmoB$_{55-414}$ protein grown from the host *E. coli* K12 TB1 cells as well as the PmoB subunit in a control consisting of the purified pMMO protein with the PmoABC from *M. capsulatus* (Bath). The PmoB subunits from the pMMO and the recombinant MBP-PmoB$_{55-414}$ proteins are clearly spotted on the SDS-PAGE gels with molecular masses at *ca*. 45 and 100 kDa, respectively (Fig. 3).

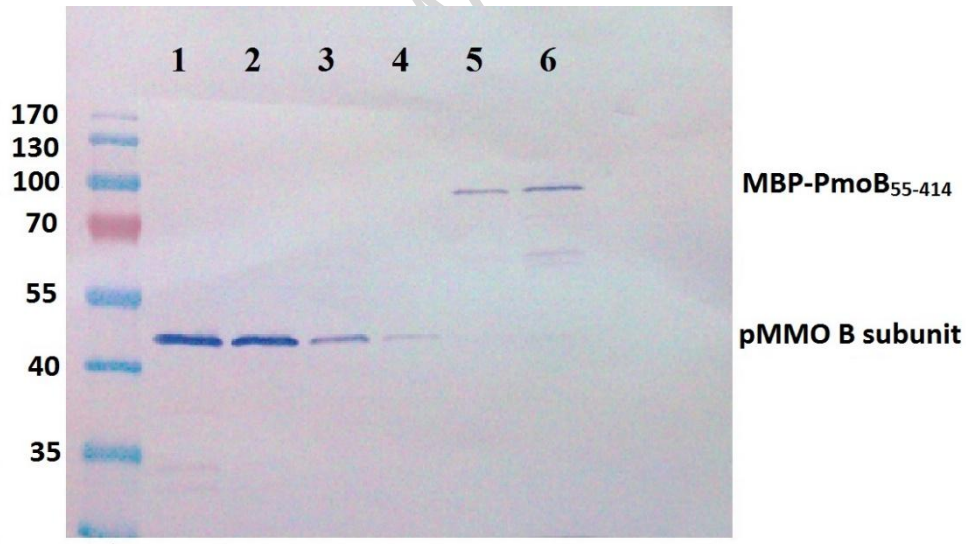

Fig. 3. SDS-PAGE/Western blotting visualization of the recombinant MBP-PmoB$_{55-414}$ from *E. coli* K12 TB1 cells and of the purified pMMO from *M. capsulatus* (Bath) using the rabbit antibodies raised against the copper-PmoB$_{55-414}$ protein (amino acid residues 55–414). The reader is referred to **Materials and Methods** section *2.4.1* for specifics on the Western blotting. Pre-stained protein markers are shown on the lane to the extreme left of the PmoB protein gels.

1. The whole cell protein extract of *M. capsulatus* (Bath) (grown in NMS buffer

containing 30 μM copper ions).

2. pMMO-enriched membranes from *M. capsulatus* (Bath).
3. pMMO-enriched membranes solubilized by DDM detergent.
4. purified pMMO complex.
5. The lysates of *E. coli* K12 TB1 cells obtained by the induction of MBP-PmoB$_{55\text{-}414}$ by IPTG (grown in the presence of 1.0 mM $CuCl_2$).
6. The membrane portion (the pellets after ultracentrifugation) of *E. coli* K12 TB1 cells obtained by the induction of MBP-PmoB$_{55\text{-}414}$ by IPTG (grown in the presence of 1.0 mM $CuCl_2$.

3.2 The MBP-PmoB fusion proteins are expressed in the cytoplasmic membranes according to immunolabeling of the bacterial cells

Armed with the antibodies, we proceed to identify the cellular location of the expressed MBP-PmoB$_{55\text{-}414}$ recombinant protein in the *E. coli* using a secondary antibody *anti* rabbit IgG conjugated with the gold nanoparticles to spot the polyclonal antibodies against the PmoB$_{55\text{-}414}$. The immunogold labeling allows us to visualize the expression of the MBP-PmoB within the *E. coli* K12 TB1 cells by TEM. The results indicate that the expression of the MBP-PmoB$_{55\text{-}414}$ protein occurs at the cytoplasmic membranes (Fig. 4), These observations are consistent with immunogold localization studies of pMMO from the denitrifying methanotroph *Candidatus Methylomirabilis oxyfera*, a species that does not develop intracytoplasmic membranes, but the pMMO resides in the cytoplasmic membranes nonetheless [27]. Note that the results highlighted in Fig. 4 are obtained on *E. coli* cells grown in 1 mM $CuCl_2$. No vacuoles are developed when the cells are grown without $CuCl_2$.

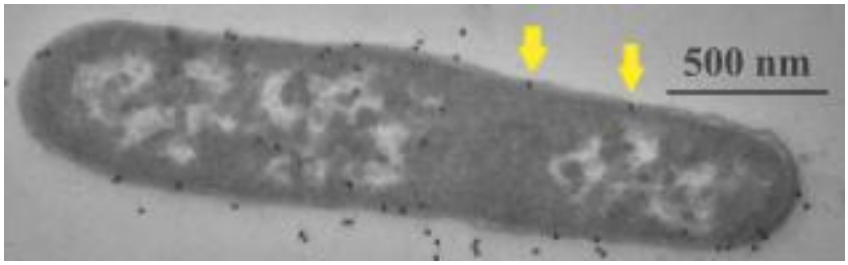

Fig. 4. TEM images of the immunogold-labeled recombinant MBP-PmoB$_{55\text{-}414}$ over-expressed in *E. coli* K12 TB1 cells (grown in the presence of 1.0 mM $CuCl_2$). The *black* dots (highlighted by *yellow* arrows) correspond to the gold nanoparticles attached to the antibodies against the copper-PmoB$_{55\text{-}414}$. The MBP-PmoB$_{55\text{-}414}$ protein is expressed in the cytoplasmic membranes of the *E. coli* cells.

3.3 Purification of the MBP-PmoB$_{55\text{-}414}$ protein and determination of the copper content

Only the MBP-PmoB$_{55\text{-}414}$ protein is sufficiently stable outside of the membranes for detergent solubilization and column chromatography. Both the full-length MBP-PmoB and MBP-PmoB$_{33\text{-}414}$ proteins aggregate when subjected to this treatment.

After detergent solubilization into DDM, the MBP-PmoB$_{55\text{-}414}$ protein can be purified to homogeneity through a MBP affinity column and its copper content determined. We quantify the PmoB-protein content by Western blotting using anti-MBP monoclonal antibody/HRP conjugates and the level of copper ions by ICP-OES. The number of coppers bound to the purified MBP-PmoB$_{55\text{-}414}$ is determined to be 6.22 ± 1.03. After removal of the MBP tag by factor Xa, the corresponding number of copper ions is 5.12 ± 0.45 per purified PmoB$_{55\text{-}414}$ protein. Thus, no more than 1 copper ion could be associated with the MBP fusion tag. As a control, we have cloned the MBP by itself in *E. coli* K12 TB1 cells and demonstrated that it binds negligible amounts of

copper.

3.4 Quantification of the MBP-PmoB proteins and the levels of copper ions in the membranes: Estimation of the copper contents of the various MBP-PmoB constructs

Although the MBP-PmoB proteins are over-expressed in the membranes, they account for only approximately 2% of the total proteins in the membranes. However, the bulk of the copper ions in the membranes are associated with the PmoB proteins. To demonstrate this, we have compared the X-ray absorption near edge spectra (XANES) in the Cu *K*-edge of the purified membranes of the *E. coli* K12 TB1 cells expressing the MBP-PmoB$_{55\text{-}414}$ protein with and without IPTG induction. Under the growth of *E. coli* cells without the induction of the PmoB expression, only a small Cu *K*-edge signal is observed for the isolated cell membranes (Fig. 5(a)). In the presence of IPTG, however, the Cu *K*-edge is significantly stronger for the membranes derived from the cells expressing the MBP-PmoB$_{55\text{-}414}$ protein. The edge jump observed for the latter is shown in Fig. 5(b). From a comparison of the edge-jumps of the Cu *K*-edges from the membranes with and without induction of expression of the MBP-PmoB$_{55\text{-}414}$ (ratio 7/1), we conclude that the MBP-PmoB$_{55\text{-}414}$ protein accounts for at least 86% of the Cu ions in these membranes. Since some basil level of MBP-PmoB$_{55\text{-}414}$ is expressed in the absence of IPTG, this percentage represents a lower limit. Only several other membrane-bound copper proteins (cytochrome *bo* oxidase, NADH dehydrogenase-2, the copper trafficking protein CopA) are known based on a genomic search [28], and these proteins contribute to these *E. coli* membranes at relatively lower levels [29].

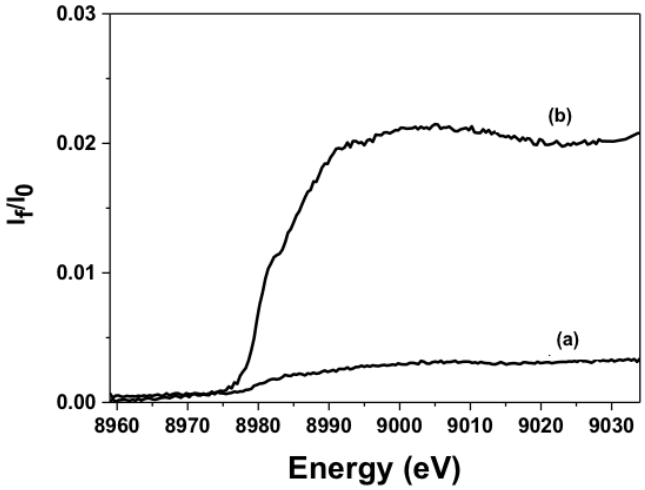

Fig. 5. The relative edge jumps of the Cu K_α near edge spectra of the cytoplasmic membranes from *E. coli* K12 TB1 strain containing the pMAL-p2X(*deSPpmob2*) plasmid without (**a**) and with (**b**) IPTG induction. The bacteria were grown with the addition of $CuCl_2$ (1.0 mM).

To quantify the MBP-PmoB protein levels within the membranes of the *E. coli* cells expressing these proteins, we have measured the PmoB-protein contents by Western blotting using anti-MBP monoclonal antibody/HRP conjugates as described earlier. Similarly, we determine the levels of copper ions in the membranes by ICP-OES. If the bulk of the copper ions in the membranes are indeed associated with the PmoB proteins, the copper contents of the various MBP-PmoB protein constructs could be assessed in this manner. These estimates provide upper limits of the copper contents since the contribution from the other copper-containing proteins in the membrane has not been accounted for. However, for a PmoB protein containing 10 copper ions, this correction would amount to no more than 1−2 copper ions, which is just outside the 10% uncertainty in the ICP-OES measurements. To illustrate, for the

membranes expressing the MBP-PmoB$_{55-414}$, we obtain 9.03 ± 2.05 for the ratio of the total copper in the membranes to the PmoB protein content. After correcting for the contribution from other copper proteins, we predict a stoichiometry of 8 ± 2 copper ions per protein, which is in essential agreement with the copper content of 6.22 ± 1.03 determined for the purified MBP-PmoB$_{55-414}$ protein, considering that 1−2 copper ions on the average have been stripped off from the protein during detergent solubilization and column chromatography.

The copper contents determined in this manner for the *E. coli* membranes expressing the various target MBP-PmoB proteins are given in Table 2. From these data, it is clear that there are as many as 9−10 copper ions associated with the full-length MBP-PmoB protein when it is expressed in *E. coli* K12 TB1 cells. As expected, *N*-truncation of the PmoB subunit results in loss of copper ions, one copper ion on the average in the case of the MBP-PmoB$_{33–414}$ protein, and possibly, an additional copper ion in the case of the MBP-PmoB$_{55–414}$ protein. In the X-ray crystal structure of pMMO from *M. capsulatus* (Bath), His48, His72 and Gln404 are ligands to the mononuclear copper at the **A** site, while His33, His137 and His139 are associated with the dicopper center at the **B** site. Thus, some loss of copper ions is anticipated upon *N*-truncation of the PmoB protein, especially in the case of the MBP-PmoB$_{55–414}$ protein with the deletion of His33 and His48. Interestingly, replacement of Tyr374 by Phe or Ser results in the loss of a total of three copper ions, suggesting the importance of Y374 in stabilizing the structure of the dicopper copper-binding domain in this mutant [30]. In any case, these Cu contents are close to the numbers of Cu ions (6–9) suggested for the E-clusters in the *intact* pMMO protein isolated from *M. capsulatus*

(Bath) [10, 12] or determined for the *C*-terminal water-exposed sub-domain of the pMMO B subunit (*ca*. 10) [20], especially when we make allowance for the three copper ions occupying the **A** and **B** sites, which we normally associate with the *N*-terminal sub-domain and have referred to as a "C-cluster".

Table 2. Copper contents of the purified $PmoB_{55-414}$ protein and of the membranes of the *E. coli* cells expressing the various MBP-PmoB proteins as quantified by ICP/OES and Western blotting.

Purified PmoB	Cu ions per protein	MBP-PmoB variants	Membrane Cu ions per protein
MBP-$PmoB_{55-414}$	6.22±1.03	$PmoB_{1-414}$	10.95±0.61
$PmoB_{55-414}$ (w/o MBP tag)	5.12±0.45	$PmoB_{33-414}$	9.54±1.00
		$PmoB_{55-414}$	9.03±2.05
		$PmoB_{55-414}$ Y374F	6.14±0.62
		$PmoB_{55-414}$ Y374S	5.93±0.57
		$PmoB_{55-414}$ M300L	8.20±0.31

3.5 The bulk of the copper ions in the membranes are Cu^I

We ascertain that the bulk of the copper ions accumulated within the membranes of the full-length MBP-PmoB as well as the *N*-truncated MBP-$PmoB_{33-414}$ and MBP-$PmoB_{55-414}$ proteins are Cu^I. The level of reduced copper ions is determined in each case on membranes (30 mg per 100 μL) suspended in Tris-HCl buffer (pH 7.0, 20 mM) using the BCA spectrophotometric method following the procedure of Yu *et al*. [20]. These Cu^I contents of the purified membranes are given in Table 3. When we

attempt to reduce any remaining copper ions in the membranes by the addition of ascorbate (final concentration 10 mM), the levels of Cu^{I} in the membranes change by less than 10%.

It is difficult to oxidize the Cu^{I} ions by O_2. This property of the reduced copper ions in the *E. coli* membranes is similar to that reported earlier for the recombinant *C*-terminal sub-domain of the PmoB in *E. coli* [20].

Table 3. The redox state of the copper ions in the recombinant full-length MBP-PmoB protein and the *N*-truncated MBP-$PmoB_{33–414}$ and MBP-$PmoB_{55–414}$ variants in their purified membranes.

MBP-PmoB proteins	Cu^{I}/Total copper
$PmoB_{1–414}$	91.1%
$PmoB_{33–414}$ (freshly prepared)	90.2%
$PmoB_{33–414}$ (incubated in air for 2 days at 4°C after preparation)	39%
$PmoB_{55–414}$	92.5%

3.6 The MBP-PmoB fusion proteins expressed in the E. coli membranes are Cu^{I}-proteins based on X-ray absorption edge measurements

We have compared the XANES in the Cu *K*-edge spectra of the various MBP-PmoB variants in the purified membranes of the *E. coli* K12 TB1 cells. In all cases, strong edge jumps are observed at 8,984 eV (Fig. 6 and Fig. S1–S3 in Supplementary Information). Comparison of the edge shifts against $CuCl_2$ indicates that the bulk of the copper ions associated with the isolated membranes must be Cu^{I} for all the MBP-PmoB fusion proteins, the same conclusion derived from spectrophotometric BCA

determination of the Cu^{I} in the purified membranes. With the large number of copper ions associated with each protein, the effect of one Cu^{II} ion out of ~10 Cu^{I} on the Cu *K*-edge would be discernible (a slight shift of ~0.1 eV). There is no apparent effect of replacing Tyr374 by Phe on the Cu *K*-edge in any of the Y374F mutants (Fig. S2 in Supplementary Information).

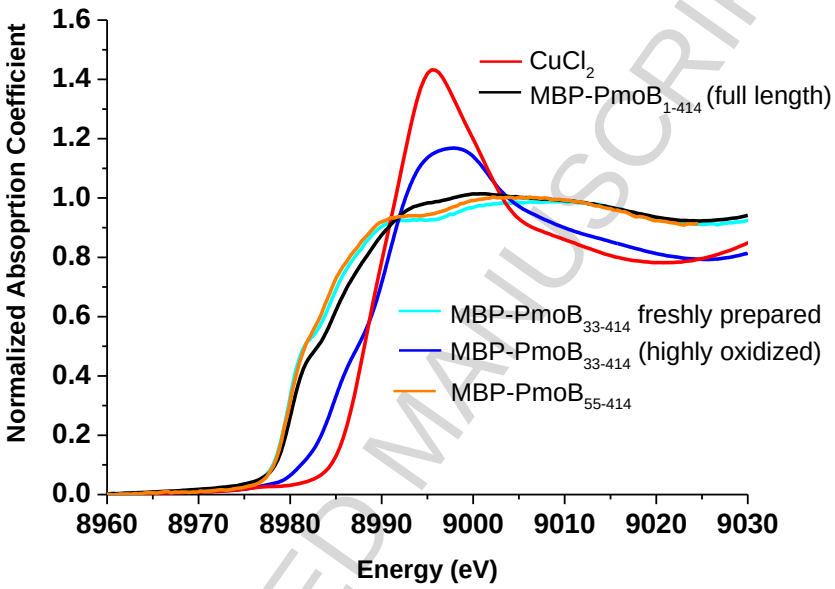

Fig. 6. Comparison of the X-ray absorption spectra of Cu *K*-edges observed for the copper ions in the membrane enriched with the full-length MBP-PmoB (*black*), MBP-$PmoB_{33-414}$ (*navy*) and MBP-$PmoB_{55–414}$ (*orange*) proteins, respectively. After exposure to air for 18–24 h at 4°C, the MBP-$PmoB_{33-414}$ protein can become almost fully oxidized (with *ca.* 20% of the Cu^{I} remaining) (in *blue*).

3.7 Effects of exposure of the MBP-PmoB proteins to air on the copper ions

The copper ions of the full-length MBP-PmoB and the MBP-$PmoB_{55-414}$ proteins are stable even after exposure to air for 48 h at 4°C. The copper ions in the membranes with these proteins stay Cu^{I} over the duration of this experiment according to the Cu

K-edge measurements. However, this is not the case with the *N*-truncated MBP-PmoB$_{33-414}$ protein. As shown in Fig. 6, the Cu *K*-edge shifts to higher energy by 2 or 3 eV, corresponding to the oxidation of about 70–80% of the copper ions in the protein. (We find that it is hard to maintain the *E. coli* membranes at *room temperature* for more than 12 h as the membranes begin to deteriorate.)

Since the bulk of the copper ions in the *E. coli* membranes with the various expressed MBP-PmoB proteins are Cu^{I}, these membranes should be EPR silent. Indeed, only very weak EPR signals (dχ″/dH) can be elicited from these membranes as isolated. Also, no new EPR signals are detected for the full-length MBP-PmoB and MBP-PmoB$_{55-414}$ proteins even after prolonged exposure to air for 24 h at 4°C. However, under a similar exposure to air, a strong EPR spectrum corresponding to 4.5 Cu^{II} ions could be discerned for the membranes of the *N*-truncated PmoB$_{33-414}$ variant (Fig. 7, *upper panel*). The number of EPR visible copper ions is consistent with the shift observed in the XANES of the Cu *K*-edge mentioned earlier.

3.8 Ferricyanide treatments of the MBP-PmoB fusion proteins in the purified membranes of the E. coli K12 TB1 cells

The EPR spectrum recorded for the membranes of the *N*-truncated PmoB$_{33-414}$ variant after prolonged exposure to air for 24 h at 4°C is a superposition of signals from different copper sites and is typical of a nearly axial square planar Cu^{II} coordination with slight rhombic distortion. Upon treatment of these oxidized copper species with 1 equiv. of $Fe(CN)_6^{3-}$ (1 equiv. = 1 protein), we see a dramatic change in the spectrum

with loss of ^{63,65}Cu nuclear hyperfine splittings in the $g_{\parallel}$ region with apparent concomitant loss of intensity corresponding to *ca.* one copper ion (Fig. 7, *upper panel*). The new signal can be assigned to the formation of a mixture of $[Fe(CN)_6^{3-}](Cu^{2+})_n$ (n = 1–4) adducts (10, 12). With further additions of $Fe(CN)_6^{3-}$ up to 10 equiv., we see additional EPR intensity corresponding to one to two additional Cu^{II} ion, suggesting oxidation of one or two Cu^{I} ions in the MBP-$PmoB_{33-414}$ to form the $[Fe(CN)_6^{4-}](Cu^{2+})$ adduct [10, 12] (Fig. 7, *lower panel*). These observations indicate that some of the Cu^{II} ions in the MBP-$PmoB_{33-414}$ protein are solvent exposed. In contrast, none of these observations are noted for membranes of the full-length MBP-PmoB and the MBP-$PmoB_{55-414}$ proteins. Only a very low level of Cu^{II} (significantly less than one Cu^{II} ion) is detected for membranes of the full-length MBP-PmoB and the MBP-$PmoB_{55-414}$ proteins. This difference in behavior of the PmoB variants towards oxidation by O_2 or $Fe(CN)_6^{3-}$ is dramatic. The EPR intensities obtained from double integration of the EPR spectra are summarized in Table S1 in Supplementary Information.

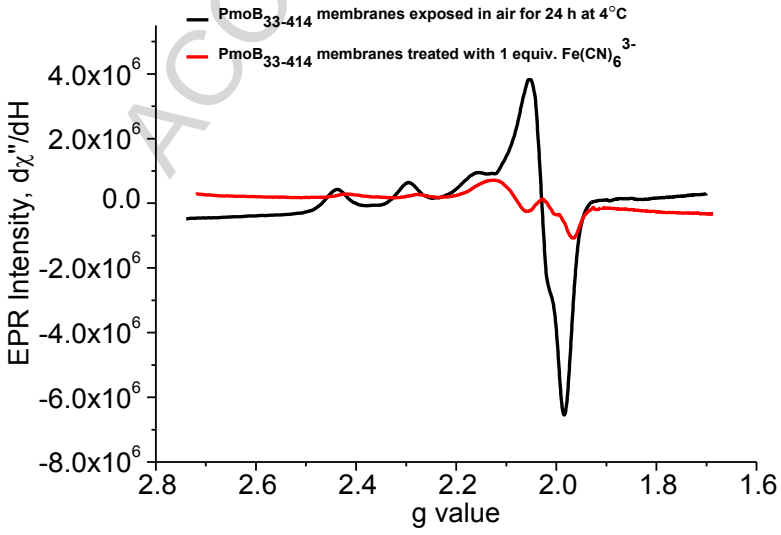

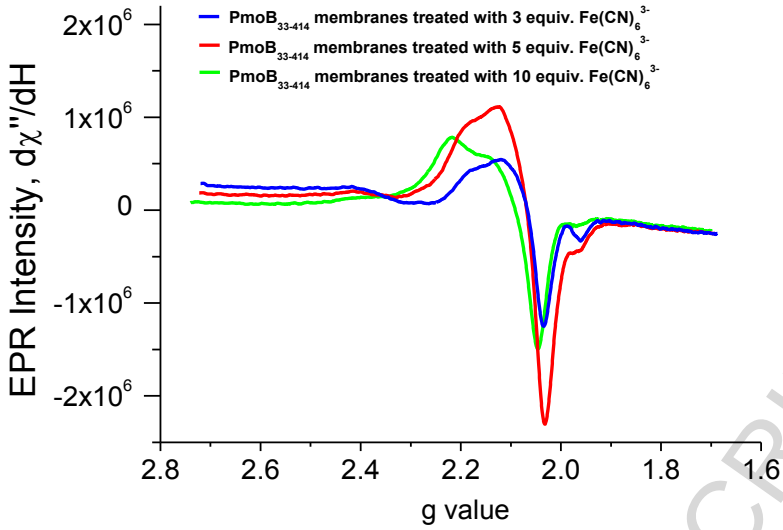

Fig. 7. EPR spectra of the purified $PmoB_{33-414}$ membranes and effects from $Fe(CN)_6^{3-}$ treatment. *Upper panel:* Comparison of the EPR spectrum obtained after the addition of 1 equiv. of $Fe(CN)_6^{3-}$ (*red*) with that of the membranes that have been exposed to air for 24 h at 4°C (*black*). *Lower panel:* EPR spectra recorded after the addition of 3, 5, and 10 equiv. of $Fe(CN)_6^{3-}$.

3.9 EXAFS of the copper ions in the various MBP-PmoB fusion proteins expressed in the membranes of the E. coli cells

EXAFS analysis of the copper ions associated with the MBP-PmoB fusion proteins can be used to develop a preliminary glimpse of the average Cu-core structure, including possible ligand types, coordination number, and average Cu-ligand distances.

For direct comparison with results reported earlier on the spmoB protein [14], we first describe our analysis on the MBP-$PmoB_{55-414}$ protein. This analysis is performed on the X-ray absorption data shown in Fig. 5(b) for purified membranes of the MBP-$PmoB_{55-414}$ protein. The latter contains about 8 Cu^{I} ions. Best fitting of the

EXAFS data suggests an average copper ion coordinated with 3 N/O at 2.11 Å, or 3 N/O at ~2.03 Å and 1 S at ~2.37 Å, when Cu–Cu scattering is not included in the analysis (Fits 7 and 8 in Table S3 and Fig. S4(e) and (f) in Supplementary Information). When we include the Cu–Cu scattering, we obtain a better goodness-of-fit factor (R_{fit} value of 0.24%) with a disorder contribution to the Debye-Waller factor corresponding to the mean-squared displacement σ^2 (Å^2)= 0.005 (Fig. 8(c) and Fit 10 in Table S3 in Supplementary Information). Best fitting of the EXAFS data with this model suggests an average copper ion coordinated with 2 N/O at 2.04 Å, 1 S at 2.37 Å, and 0.15 Cu at 2.73 Å. According to this analysis, we surmise that only 1.2 copper ions are sensing Cu···Cu back-scattering in the PmoB protein containing a total of 8 copper ions. In other words, the occupancy of the dinuclear site (the **B** site) is about 60%. The Cu···Cu distance of 2.73 Å is substantially longer than the distance of 2.53 Å reported for the dicopper site in the spmoB protein.

Two or three copper ions with a ligand structure consisting of 3 or 4 N/O coordinated at 1.95 Å and 0.25 Cu at 2.53 Å have been inferred from analysis of the EXAFS data on the spmoB protein [14]. In this earlier work, there is no evidence of a strong Cu–S scattering. The E-cluster copper ions are not part of the spmoB protein, so there are many fewer copper ions contributing to the Cu *K*-edge absorption. The difference between the two preparations is that our PmoB proteins are over-expressed in the membranes of *E. coli* with Cu^{I} introduced endogenously, presumably with the assistance of the copper trafficking protein and copper metal chaperone(s) associated with the *E. coli* membranes [22, 23], whereas in the case of the spmoB, the protein is heterologously expressed in *E. coli* and the copper ions are added as Cu^{II} exogenously

[14]. Evidently, many of the Cu^{I} sites are not assembled with the latter construct.

(a) EXAFS Fit 3, $PmoB_{1-414}$ (including 0.3 Cu-Cu)

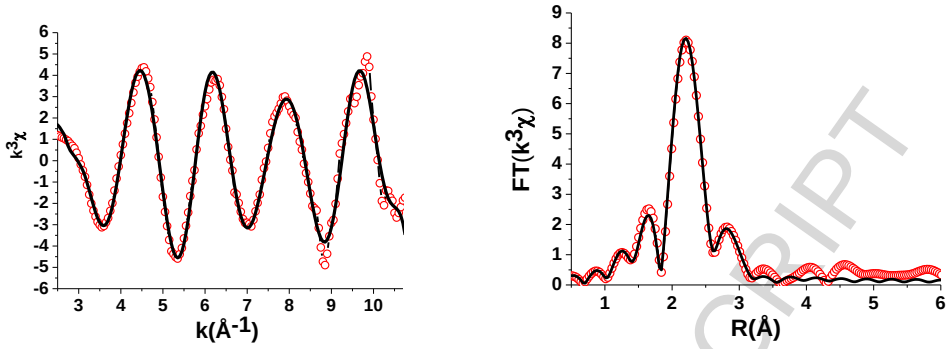

(b) EXAFS Fit 6, $PmoB_{33-414}$ (fully reduced) (including 0.4 Cu-Cu)

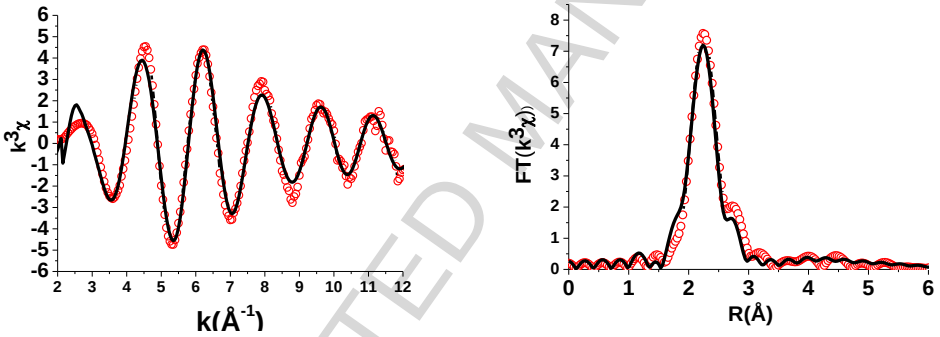

(c) EXAFS Fit 10, $PmoB_{55-414}$ (including 0.15 Cu-Cu)

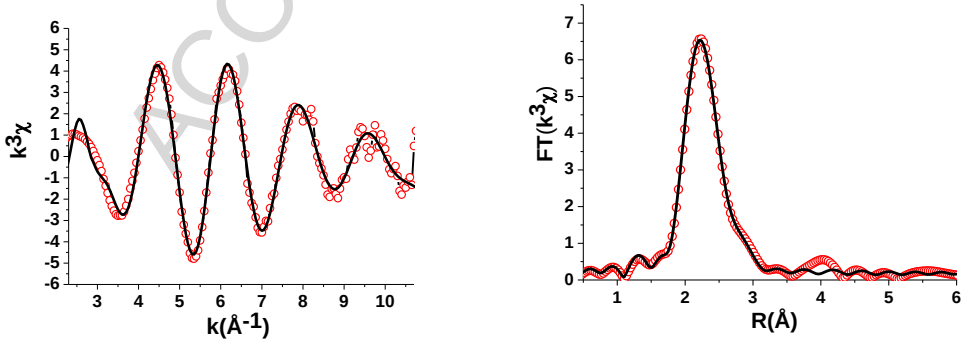

(d) EXAFS Fit 13, $PmoB_{33-414}$ Y374F Fit 3 (including 0.3 Cu-Cu)

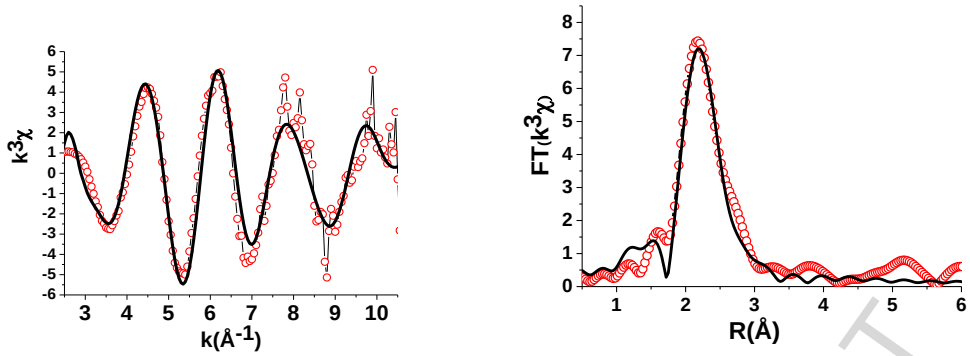

Fig. 8. The Cu EXAFS and their Fourier transforms of the MBP-PmoB proteins enriched in the cytoplasmic membranes of *E. coli* K12 TB1 cells: (**a**) the full length MBP-PmoB$_{1\text{-}414}$; (**b**) the fully reduced PmoB$_{33\text{-}414}$; (**c**) PmoB$_{55\text{-}414}$; and (**d**) PmoB$_{33\text{-}414}$ Y374F. *Left*: Cu EXAFS (*red* circles) and the corresponding best fits (*black* solid lines); *Right*: Phase shift corrected Fourier transforms of the Cu EXAFS (*red* circles) and the corresponding best fits *(black* solid lines). All the parameters used in the data fitting are provided in Table S3 in Supplementary Information.

In the present study, similar results are obtained for the membranes enriched with the full-length MBP-PmoB protein, the fully reduced MBP-PmoB$_{33–414}$ protein in the presence of ascorbate, and the MBP-PmoB$_{33–414}$ Y374F protein. The copper ions in these protein constructs are typically fully reduced. For these proteins, the first shell data (2.0 Å < R < 3.0 Å) in the Fourier transforms of $k^3\chi$ mainly arises from the back-scattering from ~3 ligated N/O atoms with the average distance of 2.09–2.11 Å. (Fig. S4 and Table S3 in Supplementary Information). Including one additional Cu–S back-scattering at a distance of 2.31–2.37 Å can significantly improve the quality of the data fitting, lowering R_{fit} below 2%, the threshold of the confidence level. The Cu–O/N back-scatterers distances are then shortened to 2.03–2.05 Å. (Fig. S4 and Table S3 in Supplementary Information). When we include Cu–Cu scattering, we obtain an even

much better goodness-of-fit, except in the case of $PmoB_{33-414}$ Y374F (Table S3). The contribution of the Cu···Cu scattering to the EXAFS varies from system to system, with coordination numbers of 0.3–0.4 and Cu···Cu distances in the range 2.64–2.95 Å (Fig. 8 and Table S3 in Supplementary Information). The Cu···Cu scattering contribution to the EXAFS decreases from 100% occupancy of the dicopper site in the membranes of the full-length MBP-$PmoB_{1–414}$ protein to *ca.* 60% in the case of the MBP-$PmoB_{55–414}$ protein.

Interestingly, upon exposure of the MBP-$PmoB_{33–414}$ membranes to air for 24 h at 4°C, we can fit the EXAFS data using the mononuclear and dinuclear copper core with the histidine coordination (**A** and **B** sites) inferred from the X-ray crystal structure of pMMO of *M. capsulatus* (Bath) [7, 14, 31] as a structural model for these three copper ions. The best fit of the first shell fitting (1.9 Å < R < 3.0 Å) to the Cu EXAFS data yields an average copper ion with a ligand structure of 3–4 O/N atom (1.95–1.97 Å) and 1 S atom (2.26–2.49 Å) (Fig. 9, Fig. S5 and Table S4 in Supplementary Information). The distances for the Cu–O/N scattering are shorter, and the distance corresponding to the Cu–S scattering has been lengthened significantly, a geometry that is more consistent with a typical Cu^{II} ion. A strong Cu···Cu back-scattering feature with a contribution from two coppers at 2.79–3.13 Å also develops in the Fourier transformed amplitudes FT[$k^3\chi(k)$] in this system (Fig. 9, Fig. S5 and Table S4 in Supplementary Information). This Cu···Cu scattering is different from that noted earlier for the fully reduced MBP-$PmoB_{33–414}$ or the full-length protein. It is also not evident in the case of the MBP-$PmoB_{33–414}$ Y374F mutant. However, it is likely that the latter protein has lost one of the copper ions from the *N*-terminal sub-domain, presumably the

copper that is coordinated to H33 (or stabilized by Y374). With additional second, third and fourth shell back-scattering from His atoms (2.0 Å < R < 4.0 Å) included in the analysis for each of the copper ions occupying the **A** and **B** sites (2–3 × 2.30–3.21 Å for Cu–C_α and 3 × 3.91–3 Å for Cu–C/N), the fitting range in *R* space can reach higher than 4.0 Å with an excellent R_{fit} (< 0.50%).

(a) EXAFS Fit 15

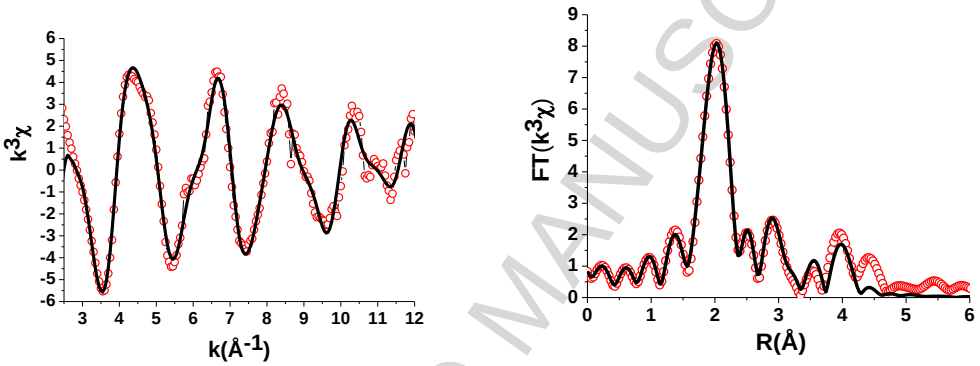

(b) EXAFS Fit 17

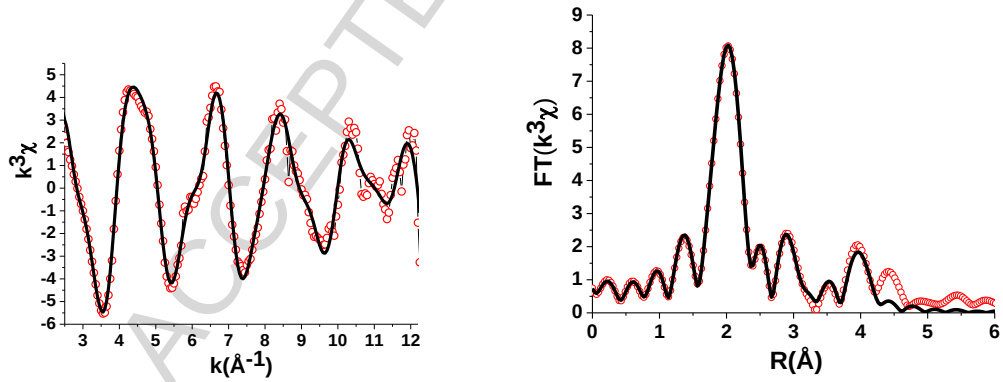

(c) EXAFS Fit 18

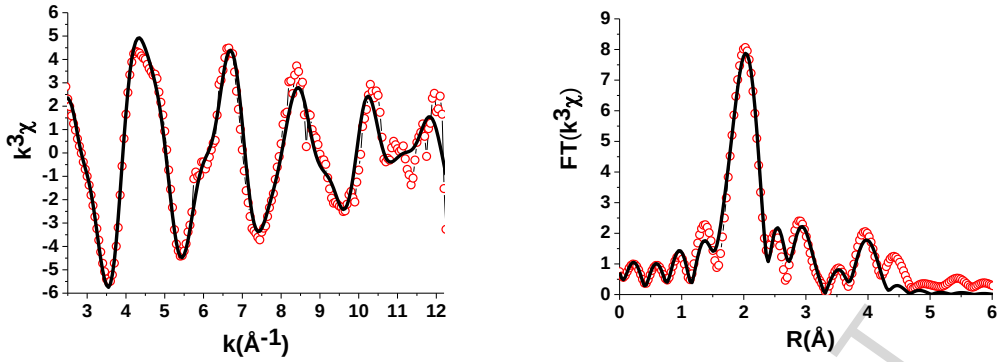

Fig. 9. The Cu EXAFS and their Fourier transforms of the MBP-PmoB$_{33-414}$ protein enriched in the cytoplasmic membranes of *E. coli* K12 TB1 cells after exposure to air for 24 h at 4°C. *Left*: Cu EXAFS (*red* circles) and the corresponding best fits (*black* solid lines); *Right*: Phase shift corrected Fourier transforms of the Cu EXAFS *(red* circles) and the corresponding best fits (*black* solid lines). (**a**)–(**c**) denote the three different better fits among the models used to fit the data, with the inclusion of Cu–S (Met), Cu–C$_\alpha$ (His), Cu–Cu and/or Cu–C/N (His) back-scatterings. All the parameters used in the data fitting are provided in Table S4 in Supplementary Information.

With 9–10 copper ions, it would not be possible to obtain unambiguous information on the ligand structure of the individual copper cofactors. Nonetheless, certain general conclusions are evident from analysis of the EXAFS data. First, the copper ions in the reduced MBP-PmoB variants display ligand structures consisting of 2–3 N/O coordinated at 2.03–2.11 Å and 0.15–0.40 Cu coordinated at 2.64–2.95 Å (Fig. 8, Fig. S4 and Table S3 in Supplementary Information). When the MBP-PmoB$_{33-414}$ becomes oxidized by air, the Cu–N/O distances are shortened to 1.95–1.97 Å (Fig. 9, Fig. S5 and Table S4 in Supplementary Information). Taken together, these data are consistent with an earlier EXAFS study on a preparation of pMMO containing only 2–3 copper ions per protein, which also showed a lengthening of the average Cu–N/O bond lengths upon reduction of the copper ions, concomitant with the increase of the Cu–Cu distance

from 2.51 to 2.65 Å [31]. A more recent Cu EXAFS study of the as-isolated pMMO has revealed also primary coordination of 2 N/O ligands at 2.09 Å and 0.3 Cu coordinated at 2.66 Å [14]. We offer these comparisons here to lend support to the presumption that the Cu^{I} ions observed in the present study of the recombinant membrane-bound PmoB variants are indeed related to the PmoB subunit in the intact pMMO. Second, many of the copper ions must have a ligand coordination consisting of 2–3 N/O and 1 S, with the latter coming from a Met S given the Cu–S distance of ~2.36 Å and the high reduction potential of these copper ions. The PmoB subunit is unique with its propensity of Met residues, as well as the abundant number of Glu and Asp residues (Table S2 in Supplementary Information). Third, there are a pair of copper ions that are in sufficiently close proximity for Cu···Cu back-scattering in the Cu EXAFS, with a Cu···Cu distance of ~2.7 Å in the reduced state and the capability to form a well-defined μ-(η^2:η^2)-peroxo dicopper (II) or a bis-(μ-oxo)-dicopper(III) structure, presumably with a Cu···Cu distance >3.0 Å [32−35], upon reaction with O_2, as observed upon exposure of the MBP-$PmoB_{33–414}$ membranes to air. One of these copper ions are presumably associated with His33 in the *N*-terminal sub-domain, though the involvement or participation of Y374 from the *C*-terminal sub-domain cannot be ruled out (Fig. 10) [30]. In any case, we see oxidation of copper ions only in the case of the MBP-$PmoB_{33–414}$, not for the full length MBP-PmoB protein, even though there is evidence for Cu···Cu back-scattering in the Cu *K*-edge EXAFS spectrum of the full-length MBP-PmoB membranes, with an average coordination number of 0.30 and a Cu···Cu distance of 2.70 (R_{fit} = 0.11%), or a total occupancy of two copper ions (Fit 3 in Table S3 and Fig. 8(a)). Evidently, the details of the dicopper site must be dependent on

whether or not the leader sequence is part of the *N*-terminal sub-domain, whether or not the Y374 plays a role in this structure, and any O_2 chemistry is associated with the site.

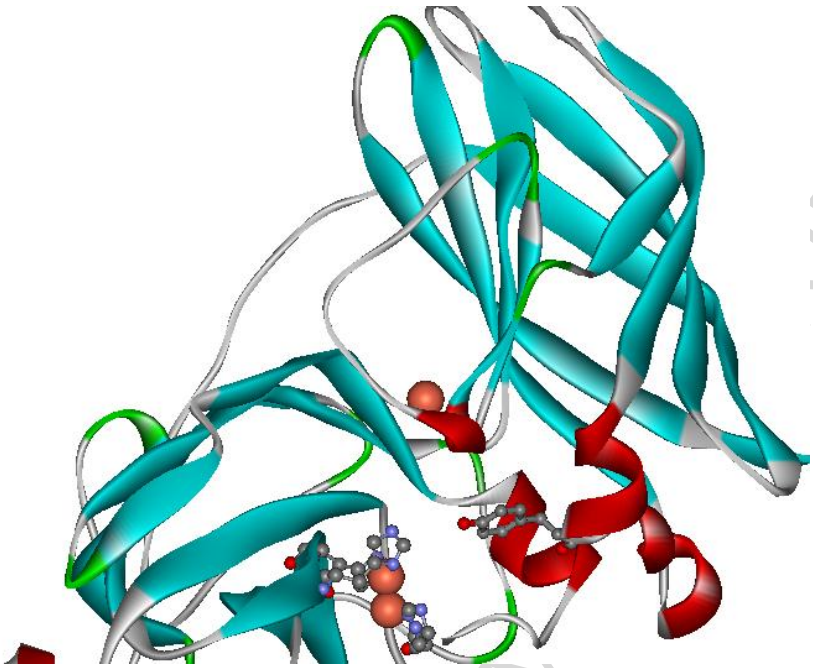

Fig. 10. The two coppers located at the **B** site of the PmoB subunit according to the X-ray crystal structure of pMMO reported by R. L. Lieberman, A. C. Rosenzweig [7], with His33, His137, His139, and Tyr374 highlighted. The single copper ion occupying the mononuclear **A** site is also shown at the top.

3.10 Measurements of specific activities toward hydrocarbon oxidation mediated by the MBP-PmoB fusion proteins expressed in the E. coli membranes

We have examined the specific activities of our *E. coli* membranes with the various expressed MBP-PmoB proteins for their abilities to hydroxylate methane to methanol and epoxidize propene to propylene oxide at 45°C. No activity is observed for methane oxidation mediated by the *E. coli* membranes with either the expressed

MBP-PmoB$_{33–414}$ or the MBP-PmoB$_{55–414}$ proteins, regardless of whether duroquinol (0.35 M) or NADH (5 mM) is used as the reductant to drive the catalytic turnover. No chemical conversion of propene is detected with NADH (5 mM) as well. However, we find that propene is converted to acrolein quite efficiently both in the cases of MBP-PmoB$_{33-414}$ and MBP-PmoB$_{55-414}$ enriched membranes when the catalytic turnover is driven by 0.35 M duroquinol (Table S5). However, these specific activities do not correspond with the copper contents of the recombinant PmoB variants. We surmise that the production of acrolein from propene is mediated by varying amounts of Cu_2O [36] that might be sequestered by the lipid headgroups of the *E. coli* membranes.

3.11 Production of H_2O_2 by the E. coli membranes enriched with the MBP-PmoB proteins

Interestingly, we observe significant production of H_2O_2 with the MBP-PmoB$_{33-414}$ membranes, the *N*-truncated PmoB mutant that reacts with O_2 or air (Fig. 11). We incubate these membrane suspensions in air at 4°C and measure the amounts of H_2O_2 released at hourly intervals by QUANTOFIX Peroxide 25 test strips. (The H_2O_2 production is quite facile under physiological conditions. Accordingly, we have monitored the production of H_2O_2 at 4°C in order to examine the process more deliberately.) The amounts of H_2O_2 detected peak after 6 h of incubation and correspond to 5−10 mg L^{-1}; when the incubation is continued for another 2 h, the amounts of H_2O_2 detected drop to *ca*. 2−2.5 mg L^{-1}, indicating decomposition of the H_2O_2 produced with time, as expected. Based on the amounts of the recombinant

MBP-PmoB$_{33-414}$ protein in the membranes, the H_2O_2 detected after 6 h incubation corresponds to 2.8 molecules per PmoB$_{33-414}$, which would require draining *ca*. 6 reducing equivalents from the PmoB protein. Minor production of H_2O_2 is detected in the case of the MBP-PmoB$_{55-414}$ protein only when these membranes are incubated up to 25 h. We do not observe any H_2O_2 generated by the membranes enriched with the full-length MBP-PmoB protein.

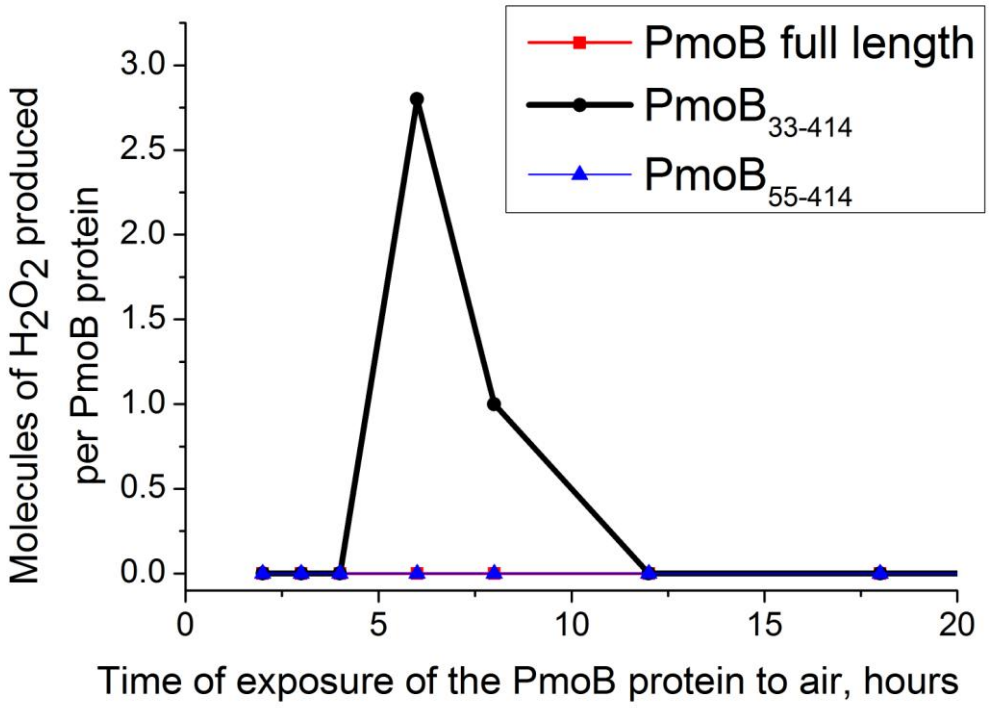

Fig. 11. Time course of the production of H_2O_2 from the MBP-PmoB enriched membranes upon incubation of the membrane suspensions in air at 4°C.

4. DISCUSSION

The structure of pMMO is enormously complex. Although crystal structures of the

pMMO from several species have been known for some years, we have, at this juncture, only the protein fold with 2 or 3 copper ions in the PmoB subunit and a Zn^{2+}/Cu^{2+} site in the PmoC subunit [7, 16, 17]. After years of debate, it is becoming increasingly evident that the catalytic site of the enzyme is a unique tricopper cluster embedded within the transmembrane domain sequestered by residues from the other two subunits, namely, PmoA and PmoC [19, 24]. The three copper ions forming the tricopper cluster were lost during the purification of the protein for crystallization and X-ray analysis [3, 6, 13]. In addition to the three copper ions that form the **A** and **B** sites, there are still many copper ions associated with the PmoB subunit [2, 3, 10, 20].

In this study, we have developed a strategy that is capable of expressing and assembling the PmoB subunit with all the copper ions in the membranes of a bacterial host cell. This approach has allowed us to undertake a more in-depth scrutiny of the different copper centers: the mononuclear copper (**A** site), the copper ions that form the dicopper center (**B** site) as well as the remaining copper ions that have been implicated in the *C*-terminal sub-domain of the PmoB subunit. To accomplish this, we have cloned and over-expressed in the membranes of *E. coli* K12 TB1 cells, the full-length PmoB protein, two *N*-truncated PmoB proteins, and several of their mutants, as fusion proteins to the maltose-binding protein. As a copper tolerant strain, the *E. coli* K12 TB1 cells might be equipped with the copper trafficking protein Cop A to insert Cu^{I} ions into a membrane-bound protein subunit [20, 21, 37], if these Cu^{I} ions were intended to be part of the protein-structure design with a specific function in mind.

Indeed, one of the most significant findings that have emerged from the present work is that the PmoB subunit is a Cu^{I} protein with many copper-binding sites. This is

the case for all the MBP-PmoB proteins expressed in the membranes. Second, the functioning PmoB protein contains as many as 9−10 copper ions, as previously reported for the PmoB subunit in the *holo* pMMO [1, 2, 10−12]. In addition to the three total copper ions occupying the **A** and **B** sites in the *N*-terminal sub-domain, there are *ca*. 6−7 Cu^{I} associated with the *C*-terminal sub-domain of the PmoB subunit.

It has been reported that the recombinant spmoB protein with the dinuclear copper site (the **B** site) is capable of oxidizing methane to methanol and propene to propylene oxide in the presence of O_2. In the activity assays, a high dose of duroquinol (1.0 M) is supplemented to provide the reducing equivalents for the chemical transformation. Although these activities are low, 0.0302 ± 0.0105 and 0.2031 ± 0.0202 $min^{-1}protein^{-1}$ for the epoxidation of propene to propylene oxide and conversion of methane into methanol, respectively [1−3, 14], these observations are quite remarkable, especially given that no specific activity toward methane oxidation or propene epoxidation has been observed for any of the MBP-PmoB proteins in the present study. We surmise that the different reactivity of our PmoB constructs and the spmoB protein toward O_2 and methane oxidation arises from the different interactions between the Cu^{I} ions occupying the **A** and **B** sites in the PmoB and spmoB constructs under these conditions. In the membrane-bound PmoB subunit, the *N*-terminal and *C*-terminal sub-domains are anchored in the membrane and the **A** and **B** site copper ions are constrained to facilitate ligation of the Cu^{I} at the **A** site with Gln404 from the *C*-terminal sub-domain. In the case of the spmoB construct, the *N*- and *C*-terminal domains are linked by only a short Gly-Lys-Gly-Gly-Gly (GKGGG) linker and the coordination of the Cu^{I} at the **A** site with Gln404 is disrupted. With the reduction

potential of this copper atom lowered significantly, the Cu^{I} ion can readily provide a reducing equivalent to the dicopper center at the **B** site nearby when the latter reacts with O_2. Thus, with three reducing equivalents readily available, the copper ions occupying the **A** and **B** sites can function together as a "tricopper cluster" and harness an "oxene" for O-atom transfer to a hydrocarbon substrate. In any case, the different catalytic behavior between the MBP-$PmoB_{33\text{-}414}$ protein and the pMMO enzyme toward hydrocarbon oxidation would argue against the active site of the functioning pMMO enzyme residing at the dicopper center (**B** site). Moreover, the methane oxidation and propene epoxidation activities observed with the spmoB variant are linked only to oxidation of duroquinol, which is not a natural substrate for pMMO.

Interestingly, the copper ions that form the **B** site in the MBP-$PmoB_{33–414}$ protein can be oxidized to Cu^{II} and produce H_2O_2 after exposure of these purified membranes to air overnight at 4°C. Concomitant with the oxidation of these copper ions, we detect Cu···Cu back-scattering in the Cu EXAFS of the MBP-$PmoB_{33–414}$ protein just as has been reported for the spmoB protein by the Northwestern group [14]. Almost all the E-cluster copper ions are also oxidized by this treatment, releasing 2.8 molecules of H_2O_2 per PmoB protein.

Although it is apparent that the copper ions occupying the **A** and **B** sites in the full length MBP-$PmoB_{1–414}$ protein cannot be oxidized in the presence of air, we do observe a Cu···Cu backscattering contribution, corresponding to total occupancy of a dicopper site to the Cu EXAFS in the fully reduced full-length MBP-PmoB protein. Similarly, the MBP-$PmoB_{55\text{-}414}$ protein remains fully reduced upon exposure to air (Fig. 6), but the Cu EXAFS for these membranes are well fitted with a Cu···Cu back-scattering

contribution corresponding to 60% occupancy of the dicopper site (Fig. 8(c)). In fact, regardless of whether the PmoB subunits are expressed with the amino acid residues 1–414, 33–414, or 55–414, Cu···Cu back-scattering is observed for the recombinant as-isolated MBP-PmoBs in the *E. coli* membranes, all comparable to the recent EXAFS data reported on pMMO in its reduced and as-isolated forms [14, 31]. Thus, it is evident that the various variants of the PmoB subunit fused with MBP that we have heterologously over-expressed in the *E. coli* membranes can serve as a functional model for the study of the PmoB subunit in pMMO. If so, the **B** site is indeed a dicopper center and not a mononuclear site as recently proposed [16]. In the re-interpretation of the X-ray data, it has been tacitly assumed that the X-ray structure corresponds to that of the functional pMMO. Many copper atoms are lost using the procedure developed by Rosenzweig et al. to purify the protein for crystallographic analysis [3, 6], and it is conceivable that one of the copper atoms at the dicopper **B** site could be stripped off as well.

We stress that we see the dicopper center for all the MBP-PmoB fusion proteins, and our evidence is based on the number of Cu^{I} atoms associated with the *N*-terminal domain and the Cu···Cu backscattering contribution to the EXAFS. There is an apparent correlation between these two observables in the EXAFS data. The Cu···Cu distance varies from 2.64 Å to 2.95 Å, which is significantly longer than that for Cu^{0} nanoparticles (2.56 Å to 2.58 Å) [38] and Cu foil (2.54 Å (EXAFS) and 2.556 Å (X-ray diffraction)) [39], two potential sources of artefacts in the EXAFS experiments, where the errors for distances from the EXAFS data are estimated to be 0.01–0.03 Å.

We further emphasize that, with the MBP and the intervening linker attached to the *N*-terminus, the structure of the dicopper center in the MBP-PmoB$_{33-414}$ fusion protein differs from that in the PmoB protein of the functional *holo* pMMO. The dicopper center in our MBP-PmoB$_{33-414}$ protein is presumably formed by His137 and His139 ligated to one of the Cu^{I} ions and His33 with the other Cu^{I} (Tyr374 might be also involved here). The His33 coordination clearly encompasses one of the imidazole ring nitrogens, but possibly the peptide nitrogen of this histidine is interacting as well. The latter is not the same as the histidine brace associated with the free amino group of a *N*-terminal histidine. The free amino group of the latter is significantly more basic than the peptide nitrogen of the histidine residue. However, if the dicopper center is formed with the MBP-PmoB$_{33-414}$ construct, it should be also formed with the native PmoB subunit in pMMO without the leading sequences, in fact, with even greater stability. So it seems that the evidence for association of a dicopper center with PmoB is not an issue.

The MBP-PmoB$_{33-414}$ protein differs from the full-length MBP-PmoB protein in that the *N*-terminal leader sequence is not included in the *N*-truncated sequence. As a leader sequence, these amino acids should not be part of the functional pMMO, and in fact,

this part of the PmoB sequence does not appear in the X-ray structures of the pMMO proteins reported to date [7, 15, 18]. Given the different reactivity between the MBP-PmoB$_{33-414}$ and full-length MBP-PmoB proteins towards O_2, there must be a structural basis for the dramatic difference in the biochemistry. Since the dicopper site must open up before it can react with O_2, it is evident that excision of the leader sequence introduces structural flexibility to this part of the protein. In other words, the dicopper site could be part of a conformational switch that responds to O_2. As further evidence of this structural flexibility, with further truncation of the *N*-terminal sub-domain to delete residues 33 to 54 to form the MBP-PmoB$_{55-414}$ construct, it is apparent that the Y374 stabilizes the protein structure in this region by substituting for His33. Interestingly, the MBP-PmoB$_{55-414}$ variant shares more or less the same number of copper ions as the MBP-PmoB$_{33-414}$ protein even when H33 is no longer part of the construct (see Table 2). Thus, we surmise that Y374 stabilizes the copper normally associated with H33 and transforms the "binuclear" site into two uncoupled mononuclear centers so that the two coppers occupying the **B** site are now too constrained to react with O_2. We would expect the loss of this copper ion (possibly together with the other copper ion at the **B** site and the mononuclear copper at the **A** site)

when Y374 is replaced by phenylalanine or serine. Indeed, we observe the loss of a total of *ca*. 3 coppers from the full-length MBP-PmoB protein in the corresponding MBP-PmoB$_{55\text{-}414}$ Y374F and Y374S mutants.

The remaining Cu^{I} ions of the PmoB subunit, *ca*. 6 or 7 in number, have very high redox potentials and cannot be oxidized directly by O_2. However, in a scenario in which the copper ions associated with the **B** site can react with O_2, as in the case of the membranes of the MBP-PmoB$_{33\text{-}414}$ protein, it is evident that these reducing equivalents can be gradually drained away from the E-cluster Cu^{I} ions. We surmise that the reaction of O_2 with the dicopper site can gate the flow of reducing equivalents from these Cu^{I} ions to produce the H_2O_2 observed.

Thus the PmoB subunit of pMMO might not only be a Cu^{I} sponge, namely just a reservoir of reducing equivalents for the turnover of the pMMO enzyme. The PmoB subunit can also be mechanically malleable. Examination of the PmoB amino acid sequence shows that the subunit is extremely rich in Met, Asp, and Glu (Table S2 in Supplementary Information), with many of these related residues even only one or two residues apart. With the large number of these hard ligands and the spatial distribution of these amino acids within the protein fold, it is possible to vary the ligand structures of the 6 or 7 copper ions with a small expenditure of conformational energy. If so, it might be possible to exploit conformational linkage between the PmoB *N*-terminus and the transmembrane domain, including both the PmoA and PmoC subunits, to activate

the dinuclear cluster for O_2 binding at the **B** site during turnover of the enzyme. The subsequent O_2 chemistry at the dicopper site can then change the conformation of the PmoB subunit and tune the redox potentials of the copper ions by a simple replacement of ligands, *e.g.*, substituting the Met by N/O of Asp or Glu. In this manner, the enzyme can gate the flow of electrons from the PmoB subunit to the catalytic site embedded within the transmembrane domain during turnover. The Cu EXAFS structural differences that we have observed between the fully reduced full-length MBP-PmoB protein and the "fully oxidized" MBP-PmoB$_{33–414}$ protein clearly indicates that this scenario is plausible. If so, the PmoB subunit can behave as a free energy transducer, the free energy for the mechanical-electrical transduction deriving from the free energy of O_2 binding to the two copper ions at the **B** site as well as the O_2 chemistry, augmented by interactions of the PmoB subunit with the PmoA/PmoC subunits. Although at this juncture we have no data that bears on the role of the mononuclear Cu^I at the **A** site in the overall function of the enzyme, it is conceivable that this copper ion can participate, at least in part, in the allosteric linkage between the *N*- and *C*-terminal sub-domains of the PmoB subunit to accomplish the mechanical-electrical transduction elicited by the dioxygen chemistry at the **B** site mentioned above. Interestingly, the ligands of this Cu^I ion are associated with amino acid residues from both the *N*- and C-terminal water soluble sub-domains (His38, His72 and Gln404) of the PmoB subunit [7].

Earlier we invoked inter-cluster electron transfers between the E-cluster copper ions and the catalytic site as a way to complete the catalytic cycle during turnover of the pMMO [6, 13]. With the possibility of tuning the ligand structures of the E-cluster

copper ions by the O_2 chemistry at the **B** site in the PmoB subunit, it seems that these inter-cluster electron transfers are feasible, despite the high reduction potentials of these copper ions in the resting state of the enzyme. However, another possibility in terms of mechanism is that the O_2 chemistry at the "dicopper" site is primarily intended to generate the μ–(η^2:η^2)-peroxo dicopper(II) species, as in polyphenol oxidases like tyrosinases and catechol oxidases [40−41], followed by release of a H_2O_2 molecule into a substrate/product channel leading to the catalytic site upon the uptake of two protons. This H_2O_2 molecule could be used to regenerate the tricopper $Cu^ICu^ICu^I$ catalytic site embedded within the transmembrane domain during turnover of the pMMO, by providing the two reducing equivalents required to reduce the $Cu^ICu^{II}(O)Cu^{II}$ tricopper species formed after O-atom transfer to the hydrocarbon substrate from the activated tricopper catalyst during the oxidative phase of the catalytic cycle. The two protons needed to form the H_2O_2 reductant would come from the water/proton channel(s) within the enzyme formed by the many Asp/Glu lining the interface between the PmoA and PmoB subunits. This same strategy (Scheme 1) has recently been used to regenerate the tricopper catalyst for multiple turnovers in the development of biomimetic tricopper complexes for selective oxidation of methane and other small alkanes under ambient conditions [19, 42-44]. In principle, the O_2 chemistry mediated by the dicopper species at the **B** site could lead to the formation of the bis-(μ-oxo)-dicopper(III) species, but this scenario would require two additional reducing equivalents from the E-cluster domain.

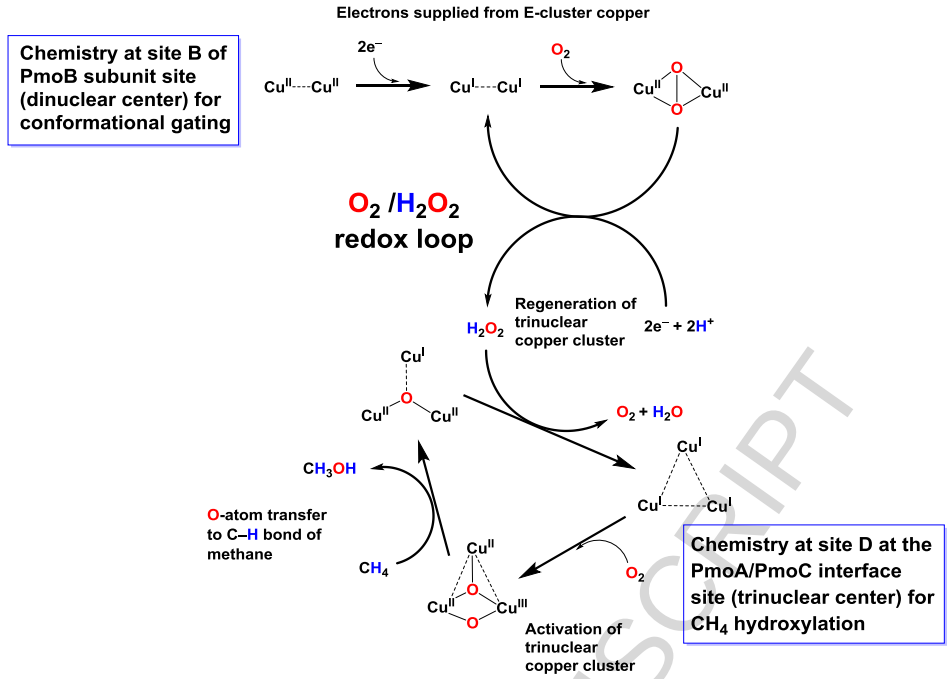

Scheme 1. Possible O_2/H_2O_2 redox loop between the dinuclear copper site (the **B** site) and the trinuclear copper site (the **D** site).

According to this picture, the turnover of the tricopper cluster at the catalytic site would be linked to the reducing equivalents stored in the E-clusters in the PmoB subunit *via* the O_2 chemistry facilitated by dicopper center at the **B** site, with the H_2O_2 produced serving as a redox mediator in a O_2/H_2O_2 redox loop. Of course, this linkage is not expected to be perfectly tight. With "molecular slippage", the conformation-gating dicopper-peroxo species formed at the **B** site, could be reduced further to give two H_2O molecules eventually; or the H_2O_2 formed and released into the substrate/product channel of the enzyme could simply diffuse away from the protein pocket to the bulk solution. Such a scenario will be wasteful of reducing equivalents and compromise the efficiency of the pMMO enzyme, but as a redox-driven "molecular machine", we must include these kinds of events in evaluating the performance of the system. Whether the catalytic cycle of pMMO involves the O_2/H_2O_2 redox loop as

conceived here, or direct electron transfers between the E-clusters and the catalytic site upon conformation gating of the PmoB subunit, or some combination of these two or other schemes, remains to be clarified. Finally, lest be there any misunderstanding, the reducing equivalents to regenerate the tricopper cluster catalyst during turnover can also come from quinols within the intracytoplasmic membrane, depending on their availability within the quinol pool [6]. The relative contribution of the two pathways is expected to depend on the level of over-expression of the pMMO in the methanotroph.

Earlier, we also proposed that two O_2 molecules are involved during the catalytic turnover of pMMO [6]. The scheme implicated here is consistent with this suggestion. However, since the regeneration of the tricopper cluster *via* reduction by H_2O_2 produces a molecule of O_2, there is only a net consumption of one molecule of O_2 during catalytic turnover. Thus, it seems that the pMMO enzyme operates as a classical monooxygenase, requiring only one O_2 molecule and two reducing equivalents per catalytic cycle.

In conclusion, the present study has led to further understanding of the role of the membrane- bound PmoB subunit and its copper ions in the structure and function of the pMMO enzyme.

Abbreviations

BCA, bicinchoninic acid; DDM, *n*-dodecyl-β-D-maltoside; *E. coli, Escherichia coli;* ECL, enhanced chemiluminescence; EPR, electron paramagnetic resonance; EXAFS, extended X-ray absorption fine structure; HRP, horseradish peroxidase; ICP-OES, inductively coupled plasma optical emission spectrometry; IPTG, isopropyl-β-D-thiogalactopyranoside; LB medium, Lucia-Bertani medium; MBP,

maltose-binding protein; *M. capsulatus* (Bath), *Methylococcus capsulatus* (Bath); NBT/BCIP, nitro-blue tetrazolium chloride/5-bromo-4-chloro-3′-indolyl phosphate *p*-toluidine salt; NMS medium, nitrate mineral salt medium; PBS, phosphate buffered saline; pMMO, particulate methane monooxygenase; PmoA, the A subunit of pMMO; PmoB, the B subunit of pMMO; PmoC, the C subunit of pMMO; PMSF, phenylmethylsulfonyl fluoride; PVDF, polyvinylidene difluoride; spmoB, the water-soluble protein containing the PmoB *N*-terminal soluble fragment (residues 33–172) tethered to the *C*-terminal fragment (residues 265–414) by a Gly-Lys-Gly-Gly-Gly (GKGGG) linker (see Balasubramanian, R.; Smith, S. M.; Rawat, S.; Yatsunyk, L. A.; Stemmler, T. L.; and Rosenzweig, A. C. (2010) *Nature* **465**, 115-119); TBS, Tris buffer saline; TBST, TBS containing 0.10% (v/v) Tween™ 20; TEM, transmission electron microscopy; XANES, X-ray absorption near edge structure; XAS, X-ray absorption spectroscopy.

Acknowledgments

This work was supported in whole or in part by Academia Sinica (AS-107-TP-ML07 and AS-KPQ-106-DDPP) and grants from the Ministry of Science and Technology, Republic of China (MOST 94-2113-M-001-016, 101-2113-M-001-007-MY3 and 104-2113-M-001-013- MY3 to S.S.F.Y.; and MOST 101-2113-M-001-013 to S.I.C)**.** We are grateful to Dr. Jyh-Fu Lee and his staffs at the National Synchrotron Radiation Research Center, Hsinchu, Taiwan, for their kind assistance with the X-ray absorption measurements. Mr. Tai-Lang Lin assisted us with the electron microscopy analyses at the EM Core Facility of the Institute of Cellular and Organismic Biology, Academia Sinica.

Appendix A. Supplementary Information

Supplementary Information to this article can be found online at http:

References

[1] H.-H.T. Nguyen, S.J. Elliott, J.H.K. Yip, S.I. Chan, J. Biol. Chem. 273 (1998) 7957-7966.

[2] S.S.-F. Yu, K.H.-C. Chen, M.Y.-H. Tseng, Y.-S. Wang, C.-F. Tseng, Y.-J. Chen, D.-S. Huang, S.I. Chan, J. Bacteriol. 185 (2003) 5915-5924.

[3] S.I. Chan, H.-H.T. Nguyen, K.H.-C. Chen, S.S.-F. Yu, Methods Enzymol. Volume 495 (2011) 177-193.

[4] P. Basu, B. Katterle, K.K. Andersson, H. Dalton, Biochem. J. 369 (2003) 417-427.

[5] D.W. Choi, R.C. Kunz, E.S. Boyd, J.D. Semrau, W.E. Antholine, J.I. Han, J.A. Zahn, J.M. Boyd, A.M. de la Mora, A.A. DiSpirito, J. Bacteriol. 185 (2003) 5755-5764.

[6] S.I. Chan, K.H.-C. Chen, S.S-F. Yu, C.-L. Chen, S.S.-J. Kuo, Biochemistry 43 (2004) 4421–4430.

[7] R.L. Lieberman, A.C. Rosenzweig, Nature 434 (2005) 177-182.

[8] A.S. Hakemian, A.C. Rosenzweig, Ann. Rev. Biochem. 76 (2007) 223-241.

[9] S. Maji, S.S.-F. Yu, S.I. Chan, Catalysis of methane oxidation by the tricopper cluster in the particulate methane monooxygenase and biomimietic tricopper complexes in Metalloproteins: Theory, Calculations, and Experiments, Taylor & Francis, CRC Press, 2015.

[10] H.-H.T. Nguyen, K.H. Nakagawa, B. Hedman, S.J. Elliott, M.E. Lidstrom, K.O. Hodgson, S.I. Chan, J. Am. Chem. Soc. 118 (1996) 12766-12776.

[11] S.I. Chan, V.C.-C. Wang, J.C.-H. Lai, S.S-F. Yu, P.P.-Y. Chen, K.H.-C. Chen, C.-L. Chen, M.K. Chan, Angew. Chem. Int. Ed. 46 (2007) 1992-1994.

[12] K.H.-C. Chen, C.-L. Chen, C.-F. Tseng, S.S.-F. Yu, S.-C. Ke, J.-F. Lee, H.-H.T. Nguyen, S.J. Elliott, J.O. Alben, S.I. Chan, J. Chin. Chem. Soc. 51 (2004)

1081-1098.

[13] S.I. Chan, S.S.-F. Yu, Acc. Chem. Res. 41 (2008) 969-979.

[14] R. Balasubramanian, S.M. Smith, S. Rawat, L.A. Yatsunyk, T.L. Stemmler, A.C. Rosenzweig, Nature 465 (2010) 115-119.

[15] A.S. Hakemian, K.C. Kondapalli, J. Telser, B.M. Hoffman, T.L. Stemmler, A.C. Rosenzweig, Biochemistry 47 (2008) 6793-6801.

[16] L. Cao, O. Caldararu, A.C. Rosenzweig, U. Ryde, Angew Chem Int Ed, 57 (2018) 162-166.

[17] P.P.-Y. Chen, P. Nagababu, S.S.-F. Yu, S.I. Chan, ChemCatChem 6 (2014) 429-437.

[18] S.M. Smith, S. Rawat, J. Telser, B.M. Hoffman, T.L. Stemmler, A.C. Rosenzweig, Biochemistry 50 (2011) 10231-10240.

[19] S.I. Chan, Y.J. Lu, P. Nagababu, S. Maji, M.-C. Hung, M.M. Lee, I.-J. Hsu, P.-D. Minh, J.C.-H. Lai, K.Y. Ng, S. Ramalingam, S.S.-F. Yu, M.K. Chan, Angew. Chem. Int. Ed. 52 (2013) 3731-3735.

[20] S. S.-F. Yu, C.-Z. Ji, Y.-P. Wu, T.-L. Lee, C.-H. Lai, S.-C. Lin, Z.-L. Yang, V.C.- C. Wang, K.H.-C. Chen, S.I. Chan, Biochemistry 46 (2007) 13762-13774.

[21] C.E. Santo, N. Taudte, D.H. Nies, G. Grass, Appl. Environ. Microbiol. 74 (2008) 977-986.

[22] N.J. Robinson, D.R. Winge, Ann. Rev. Biochem. 79 (2010) 537-562.

[23] D. Osman, J.S. Cavet, Copper homeostasis in bacteria, Adv. Appl. Microbiol. 65 (2008) 217-247.

[24] M.D. Pham, Y.-P. Lin, Q.V. Vuong, P. Nagababu, B.T.-A. Chang, K.Y. Ng, C.-H. Chen, C.-C. Han, C.-H. Chen, M.S. Li, S.S.-F. Yu, S.I. Chan, Biochim. Biophys. Acta 1854 (2015) 1842-1852.

[25] J. Walker, ed., The Protein Protocol Handbook, second edition, Humana Press,

2002, pp. 454-462.

[26] P.K. Smith, R.I. Krohn, G.T. Hermanson, A.K. Mallia, F.H. Gartner, M.D. Provenzano, E.K. Fujimoto, N.M. Goeke, B.J. Olson, D.C. Klenk, *Anal. Biochem.* **150** (1) (1985) 76–85.

[27] M.L.Wu, T.A. van Alen, E.G. van Donselaar, M. Strous, M.S.M. Jetten, L. van Niftrik, FEMS Microbiol. Lett. 334 (2012) 49-56.

[28] P.G. Ridge, Y. Zhang, V.N. Gladyshev, Plos ONE (2008) DOI:10.1371/journal.pone.0001378.

[29] G.-W. Li, D. Burkhardt, C. Gross, J.S. Weissman J. S., Cell. 157 (2014) 624–635.

[30] Y. Shiota, G. Juhasz, K. Yoshizawa, Inorg. Chem. 52 (2013) 7907-7917.

[31] R.L. Lieberman, K.C. Kondapalli, D.B. Shrestha, A.S. Hakemian, S.M. Smith, J. Telser, J.Kuzelka, R. Gupta, A.S. Borovik, S.J. Lippard, B.M. Hoffman, A.C. Rosenzweig, T.L. Stemmler, Inorg. Chem. 45 (2006) 8372-8381.

[32] M.A. Culpepper, G.E. Cusail III, W.A, Funderson, B.M. Hoffman, A.C. Rosenzweig, J. Am. Chem. Soc. 136 (2014) 11767−11775.

[33] L.M. Mirica, X. Ottenwaelder, T.D.P. Stack, Chem. Rev. 104 (2004) 1013−1045.

[34] E.A. Lewis, W.B. Tolman, Chem. Rev.104 (2004) 1047−1076.

[35] S. Itoh, S. Fukuzumi, Acc. Chem. Res. 40 (2007) 592−600.

[36] N.-C. Lai, M.-C. Tsai, C.-H. Liu, C.-S. Chen, C.-M. Yang, J. Catal. 365 (2018) 411-419.

[37] K.J. Waldron, N.J. Robinson, Nat. Rev. Microbiol. 7 (2009) 25-35.

[38] W.C.M. Gomes, A.O.W. Neto, P.M. Pimentel, D.M.A. Melo, F.R.G. Silva, Colloids and Surfaces A: Physicochem. Eng. Aspects 426 (2013), 18–25.

[39] A. Mishra, N. Parsai, B.D. Shrivastava, Indian J. Pure. Appl. Phys. 49 (2011) 25-29.

[40] H. Decker, F. Tuczek, Trends. Biochem. Sci. 25 (2000) 392–397.

[41] E. Monzani, L. Quinti, A. Perotti, L. Casella, M. Gulotti, L. Randaccio, S. Geremia, G. Nardin, P. Faleschini, G. Tabbi, Inorg. Chem., 37 (1998) 553–562.

[42] P. Nagababu, S.S.-F. Yu, S. Maji, R. Ramu, S.I. Chan, Catal. Sci. Technol., 4 (2014) 930–935.

[43] C.-C. Liu, C.-Y. Mou, S.S.-F. Yu, S.I. Chan, Energy Environ. Sci., 9 (2016) 1361-1374.

[44] V.C.-C. Wang, S. Maji, P.P.-Y. Chen, H.K. Lee, S.S.-F. Yu, S.I. Chan, Chem. Rev., 117 (2017) 8574-8621.

Tables

Table 1. List of the target PmoB proteins.

PmoB mutants	**Description**
PmoB	The full length PmoB protein
PmoB Y374F	The full length PmoB mutant with Tyr374→Phe
$PmoB_{33–414}$	*N*-truncated PmoB w/o residues 1−32
$PmoB_{33–414}$ Y374F	*N*-truncated PmoB mutant w/o residues 1−32 and

	Tyr 374→Phe
$PmoB_{55–414}$	*N*-truncated PmoB w/o residues 1−54
$PmoB_{55–414}$ Y374F	*N*-truncated PmoB mutant w/o residues 1−54 and Tyr374→Phe
$PmoB_{55–414}$ Y374S	*N*-truncated PmoB mutant w/o residues 1−54 and Tyr374→Ser
$PmoB_{55–414}$ M300L	*N*-truncated PmoB mutant w/o residues 1−54 and Met300→Leu

Table 2. Copper contents of the purified $PmoB_{55-414}$ protein and of the membranes of the *E. coli* cells expressing the various MBP-PmoB proteins as quantified by ICP/OES and Western blotting.

Purified PmoB	Cu ions per protein	MBP-PmoB variants	Membrane Cu ions per protein
$MBP\text{-}PmoB_{55-414}$	6.22±1.03	$PmoB_{1-414}$	10.95±0.61

$PmoB_{55-414}$ (w/o MBP tag)	5.12±0.45	$PmoB_{33-414}$	9.54±1.00
		$PmoB_{55-414}$	9.03±2.05
		$PmoB_{55-414}$ Y374F	6.14±0.62
		$PmoB_{55-414}$ Y374S	5.93±0.57
		$PmoB_{55-414}$ M300L	8.20±0.31

Table 3. The redox state of the copper ions in the recombinant full-length MBP-PmoB protein and the *N*-truncated MBP-$PmoB_{33–414}$ and MBP-$PmoB_{55–414}$ variants in their purified membranes.

MBP-PmoB proteins	**Cu^{I}/Total copper**
$PmoB_{1–414}$	91.1%
$PmoB_{33–414}$ (freshly prepared)	90.2%
$PmoB_{33–414}$ (incubated in air for 2	39%

days at 4°C after preparation)	
$PmoB_{55–414}$	92.5%

Figure legends

Fig. 1. X-ray crystal structure of pMMO from *M, capsulatus* (Bath). The membrane topology of the PmoB subunit (*red*) is highlighted *vis a vis* the PmoA (*yellow*) and PmoC (*green*) subunits. The locations of the known copper sites are shown by *blue* atoms: **A** site (mononuclear copper site); **B** site (dicopper site); **C** site ("zinc" center or second mononuclear copper site); and **D** site (the site of the putative tricopper cluster

described by the Chan laboratory [6, 10−13]).

Fig. 2. The protein construct for the full-length PmoB fused to MBP. The *N*- and *C*-terminal sub-domains of the PmoB are highlighted in *blue* and *green*, respectively, with the signal peptide (residues 1 - 32) colored in *deep blue*, and the transmembrane domain from residues 172 to 265 depicted in *red*. The linker between the MBP and the PmoB containing the Factor Xa cleavage site is shown in *magenta*.

Fig. 3. SDS-PAGE/Western blotting visualization of the recombinant MBP-PmoB$_{55\text{-}414}$ from *E. coli* K12 TB1 cells and of the purified pMMO from *M. capsulatus* (Bath) using the rabbit antibodies raised against the copper-PmoB$_{55\text{-}414}$ protein (amino acid residues 55–414). The reader is referred to **Materials and Methods** section *2.4.1* for specifics on the Western blotting. Pre-stained protein markers are shown on the lane to the extreme left of the PmoB protein gels.

1. The whole cell protein extract of *M. capsulatus* (Bath) (grown in NMS buffer containing 30 μM copper ions).
2. pMMO-enriched membranes from *M. capsulatus* (Bath).
3. pMMO-enriched membranes solubilized by DDM detergent.
4. purified pMMO complex.

5. The lysates of *E. coli* K12 TB1 cells obtained by the induction of MBP-PmoB$_{55-414}$ by IPTG (grown in the presence of 1.0 mM $CuCl_2$).
6. The membrane portion (the pellets after ultracentrifugation) of *E. coli* K12 TB1 cells obtained by the induction of MBP-PmoB$_{55-414}$ by IPTG (grown in the presence of 1.0 mM $CuCl_2$.

Fig. 4. TEM images of the immunogold-labeled recombinant MBP-PmoB$_{55-414}$ over-expressed in *E. coli* K12 TB1 cells (grown in the presence of 1.0 mM $CuCl_2$). The *black* dots (highlighted by *yellow* arrows) correspond to the gold nanoparticles attached to the antibodies against the copper-PmoB$_{55-414}$. The MBP-PmoB$_{55-414}$ protein is expressed in the cytoplasmic membranes of the *E. coli* cells.

Fig. 5. The relative edge jumps of the Cu K_α near edge spectra of the cytoplasmic membranes from *E. coli* K12 TB1 strain containing the pMAL-p2X(*deSPpmob2*) plasmid without (**a**) and with (**b**) IPTG induction. The bacteria were grown with the addition of $CuCl_2$ (1.0 mM).

Fig. 6. Comparison of the X-ray absorption spectra of Cu K-edges observed for the copper ions in the membrane enriched with the full-length MBP-PmoB (*black*), MBP-PmoB$_{33-414}$ (*navy*) and MBP-PmoB$_{55–414}$ (*orange*) proteins, respectively. After

exposure to air for 18–24 h at 4°C, the MBP-PmoB$_{33-414}$ protein can become almost fully oxidized (with *ca.* 20% of the Cu^{I} remaining) (in *blue*).

Fig. 7. EPR spectra of the purified PmoB$_{33-414}$ membranes and effects from $Fe(CN)_6^{3-}$ treatment. *Upper panel:* Comparison of the EPR spectrum obtained after the addition of 1 equiv. of $Fe(CN)_6^{3-}$ (*red*) with that of the membranes that have been exposed to air for 24 h at 4°C (*black*). *Lower panel:* EPR spectra recorded after the addition of 3, 5, and 10 equiv. of $Fe(CN)_6^{3-}$.

Fig. 8. The Cu EXAFS and their Fourier transforms of the MBP-PmoB proteins enriched in the cytoplasmic membranes of *E. coli* K12 TB1 cells: (**a**) the full length MBP-PmoB$_{1-414}$; (**b**) the fully reduced PmoB$_{33-414}$; (**c**) PmoB$_{55-414}$; and (**d**) PmoB$_{33-414}$ Y374F. *Left*: Cu EXAFS (*red* circles) and the corresponding best fits (*black* solid lines); *Right*: Phase shift corrected Fourier transforms of the Cu EXAFS (*red* circles) and the corresponding best fits *(black* solid lines). All the parameters used in the data fitting are provided in Table S3 in Supplementary Information.

Fig. 9. The Cu EXAFS and their Fourier transforms of the MBP-PmoB$_{33-414}$ protein enriched in the cytoplasmic membranes of *E. coli* K12 TB1 cells after exposure to air for 24 h at 4°C. *Left*: Cu EXAFS (*red* circles) and the corresponding best fits (*black*

solid lines); *Right*: Phase shift corrected Fourier transforms of the Cu EXAFS *(red* circles) and the corresponding best fits (*black* solid lines). (**a**)–(**c**) denote the three different better fits among the models used to fit the data, with the inclusion of Cu–S (Met), Cu–C_α (His), Cu–Cu and/or Cu–C/N (His) back-scatterings. All the parameters used in the data fitting are provided in Table S4 in Supplementary Information.

Fig. 10. The two coppers located at the **B** site of the PmoB subunit according to the X-ray crystal structure of pMMO reported by R. L. Lieberman, A. C. Rosenzweig [7], with His33, His137, His139, and Tyr374 highlighted. The single copper ion occupying the mononuclear **A** site is also shown at the top.

Fig. 11. Time course of the production of H_2O_2 from the MBP-PmoB enriched membranes upon incubation of the membrane suspensions in air at 4°C.

Scheme Caption

Scheme 1. Possible O_2/H_2O_2 redox loop between the dinuclear copper site (the **B** site) and the trinuclear copper site (the **D** site).

GRAPHICAL ABSTRACT

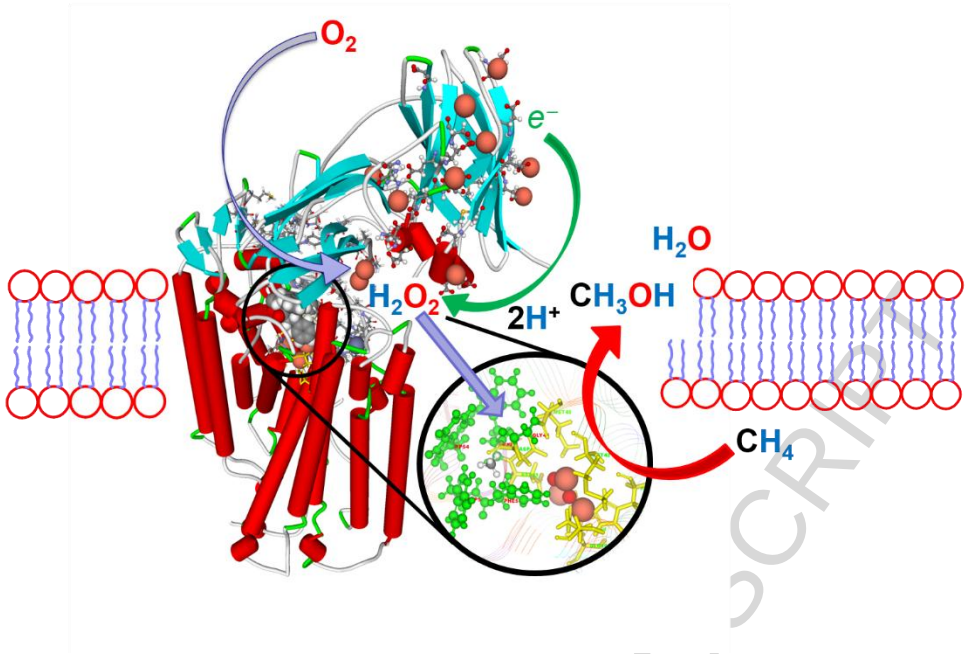

Subunit B (PmoB) of the particulate methane monooxygenase (pMMO) in *Methylococcus capsulatus* (Bath) has been cloned and over-expressed in *E. coli* K12 TB1 cells as a multicopper cytoplasmic membrane protein with *ca.* 9 Cu^{I} ions and shown to produce H_2O_2 upon reaction of O_2 with the dicopper site.

Highlights

- Subunit B (PmoB) of particulate methane monooxygenase (pMMO) is expressed in *E. coli.*
- PmoB and its variants/mutants are expressed in the membranes as Cu^{I} proteins.
- The PmoB of pMMO contains a Cu^{I} sponge with high reduction potentials for the Cu sites.
- The PmoB proteins show evidence of a dinuclear copper site.
- The PmoB-enriched *E. coli* membranes produce H_2O_2.